Journal Pre-proofs

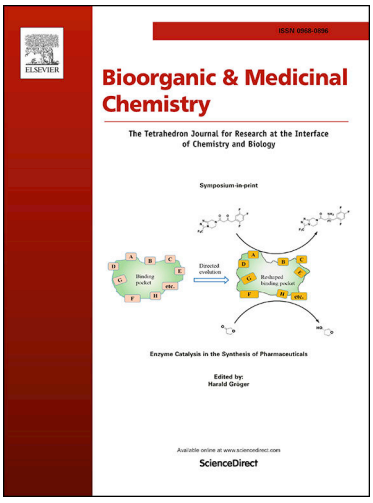

Substituted pteridinones as p90 ribosomal S6 protein kinase (RSK) inhibitors: a structure-activity study

Kimberly A. Casalvieri, Christopher J. Matheson, Donald S. Backos, Philip Reigan

PII: S0968-0896(19)31117-4
DOI: https://doi.org/10.1016/j.bmc.2019.115303
Reference: BMC 115303

To appear in: *Bioorganic & Medicinal Chemistry*

Received Date: 13 September 2019
Revised Date: 20 December 2019
Accepted Date: 31 December 2019

Please cite this article as: K.A. Casalvieri, C.J. Matheson, D.S. Backos, P. Reigan, Substituted pteridinones as p90 ribosomal S6 protein kinase (RSK) inhibitors: a structure-activity study, *Bioorganic & Medicinal Chemistry* (2020), doi: https://doi.org/10.1016/j.bmc.2019.115303

Graphical Abstract

Substituted pteridinones as p90 ribosomal S6 protein kinase (RSK) inhibitors: a structure-activity study

Leave this area blank for abstract info.

Kimberly A. Casalvieri, Christopher J. Matheson, Donald S. Backos, and Philip Reigan

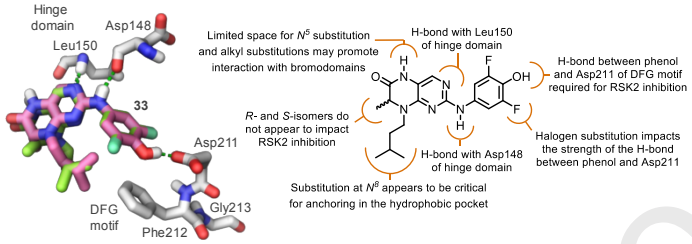

ELSEVIER

Bioorganic & Medicinal Chemistry
journal homepage: www.elsevier.com

Substituted pteridinones as p90 ribosomal S6 protein kinase (RSK) inhibitors: a structure-activity study

Kimberly A. Casalvieri[a], Christopher J. Matheson[a], Donald S. Backos[a], and Philip Reigan[a]

[a]*Department of Pharmaceutical Sciences, Skaggs School of Pharmacy and Pharmaceutical Sciences, University of Colorado Anschutz Medical Campus, 12850 East Montview Boulevard, Aurora, CO, 80045, USA.*

ARTICLE INFO

Article history:
Received
Received in revised form
Accepted
Available online

Keywords:
RSK2
kinase
inhibitor
pteridinones
cancer

ABSTRACT

The activity of p90 ribosomal S6 kinase 2 (RSK2) has emerged as an attractive target for cancer therapy due to its role in the regulation of diverse cellular processes, such as cell transformation and proliferation. Several pan-RSK inhibitors have been identified with BI-D1870 and the pseudo-analogs LJH685 and LJI308 being the most selective, potent, and frequently used small molecule inhibitors. We designed and synthesized a series of pteridinones and pyrimidines to evaluate the structural features of BI-D1870 that are required for RSK2 inhibition. We have identified inhibitors of RSK2 activity, evaluated their target engagement in cells, and measured their effect on cell viability and cytotoxicity in the MOLM-13 acute myeloid leukemia (AML) cell line. The results of our studies support that RSK2 inhibition can be achieved in MOLM-13 cells without potent cytotoxicity. The structure-activity data from this study will be used as a platform to develop novel RSK2 inhibitors.

1. Introduction

The p90 ribosomal S6 kinases (RSK1-4) are a family of serine/threonine kinases that are comprised of two functionally distinct kinase domains, a catalytic N-terminal kinase domain (NTKD) and an activating C-terminal kinase domain (CTKD) connected by a linker region. The RSK1-3 family members act as the downstream effectors of the Ras/Raf/MEK/ERK pathway,[1-4] while RSK4 has an alternative mechanism of activation.[5] Extracellular signal-regulated kinase (ERK) binds the inactive form of RSK1-3 at the C-terminal, and upon activation ERK phosphorylates serine and threonine residues in the CTKD and linker region, promoting recruitment of phosphoinositide-dependent protein kinase 1 (PDK1) that facilitates phosphorylation of the NTKD, leading to full activation of RSK.[6] The RSKs phosphorylate a range of cytoplasmic and nuclear substrates involved in transcription, translation, cell-cycle regulation, and cell survival.[1-4] Although the RSKs share a high-degree of structural homology (73–80% sequence identity), there is increasing evidence of isoform specificity in mediating diverse cellular processes.[1-4] The overall functional differences of the RSK isoforms are more apparent in cancer, with increased expression and activity of RSK1 and/or RSK2 promoting tumor growth and survival, whereas RSK3 and RSK4 act as tumor suppressors through multiple cellular mechanisms.[7] The aberrant expression and/or activity of RSKs has been associated with several cancer types, including breast cancer, colorectal cancer, head and neck squamous cell carcinoma, glioblastoma, leukemia, lung cancer, malignant melanoma, multiple myeloma, ovarian carcinoma, and prostate cancer.[8]

The Ras/Raf/MEK/ERK pathway is often activated in leukemia and confers a poor prognosis and resistance to chemotherapy.[9, 10] Activating mutations of the surface receptor kinase FMS-like tyrosine kinase 3 (FLT3) due to internal tandem duplication (ITD) are the most common abnormality in acute myeloid leukemia (AML) leading to constitutive activation of the Ras/Raf/MEK/ERK pathway.[11] More recent studies have shown that RSK2 activity is required for the initiation and progression of FLT3/ITD-induced AML.[12] Fibroblast growth factor receptor 3 (FGFR3), another tyrosine kinase cell-surface receptor, has also been implicated in the progression of hematological malignancies, including AML, by activating RSK2 via an alternative two-step mechanism facilitating ERK-RSK2 interaction and phosphorylation of RSK2.[13, 14] RSK1 and RSK2 are the predominant isoforms expressed in AML,[15] and have been reported to phosphorylate cAMP response-element binding protein (CREB), a nuclear transcription factor critical for hematopoietic cell proliferation, differentiation, and survival.[16] Approximately 60% of patients with AML express CREB at high levels and this is associated with an increased risk of relapse and decreased survival.[15] The phosphorylation of CREB by RSK1 or RSK2 promotes cell survival by increasing the transcription of Bcl-2, Bcl-xL, and induced myeloid leukemia cell differentiation

prot[illegible]lkyl small molecule inhibitors would prevent these pro-survival signaling events and be an attractive therapeutic strategy for the treatment of AML.

Several small molecule RSK inhibitors have been reported that target either the NTKD or CTKD of the RSKs. The flavonol rhamnoside SL0101 was the first pan-RSK inhibitor to be identified acting at the NTKD and several other flavanol rhamnosides have since been reported as RSK inhibitors; however, poor pharmacokinetic (PK) properties and off-target effects have limited their development.[18, 19] The fluoromethyl ketone, FMK, is a irreversible inhibitor that covalently binds to a cysteine residue in the CTKD of RSK1, RSK2, and RSK4 (the cysteine residue is absent in RSK3).[20] Although FMK is a potent and surprisingly specific RSK inhibitor, its application is limited since it is not effective once the kinase is activated and the CTKD is not always required for RSK activation.[20, 21] The reversible pan-RSK inhibitor BI-D1870 (**Figure 1**) is a dihydropteridinone that competes with ATP at the NTKD, with an *in vitro* IC_{50} of 31nM for RSK1, 24nM for RSK2, 18nM for RSK3, and 15nM for RSK4, and a concentration of ~10μM is required to completely inhibit RSK activity in cells.[22] Although some of the cell signaling effects of BI-D1870 have been attributed to non-specific interactions, it has respectable narrow-band activity within the kinome with PLK1, Aurora B, MELK, and MST2 among its other targets.[22-24] Unfortunately, BI-D1870 has a poor PK profile, displaying high clearance and a short plasma half-life and this has prevented its clinical evaluation.[25, 26] The impressive potency and selectivity of BI-D1870 led to the development of LJI308 (IC_{50} values of 3nM for RSK1, 4nM for RSK2, and 13nM for RSK3), and LJH685 (IC_{50} values of 6nM for RSK1, 5nM for RSK2, 4nM for RSK3); however, these compounds also suffer from poor PK profiles, which has limited their development and clinical utility.[27, 28]

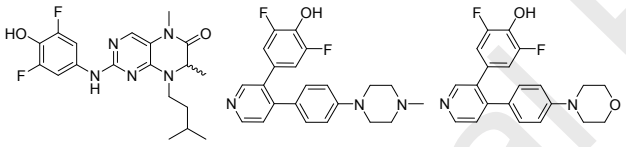

Figure 1. Chemical structures of the known RSK inhibitors BI-D1870, LJH685, and LJI308.

Despite the shortcomings of BI-D1870, it is a relatively specific and potent nanomolar inhibitor of the RSK isoforms and has been used by a number of groups to identify the physiological substrates and functional roles for RSK in cells.[22] Considering the specific and potent RSK inhibition demonstrated by BI-D1870 and the emergence of RSK1 and RSK2 as anticancer targets in multiple cancer types, it is surprising that there have been few structure-activity relationship (SAR) studies of substituted pteridinones as RSK inhibitors. The difluorophenolpyridine derivatives LJH685 and LJI308 are the only BI-D1870 analogs that have been reported and these were not developed as part of an exhaustive structure-activity study and do not interrogate substitution of the pteridinone core of BI-D1870. Therefore, we performed a SAR study to determine the necessary structural features of BI-D1870 required for RSK inhibition. Herein, we describe a series of substituted pteridinones and pyrimidines based on BI-D1870, the evaluation of their inhibition of RSK activity, and their impact on cell viability or cytotoxicity in AML cells. Our studies indicate that halogen substitutions on the 4-hydroxyanilino can greatly impact RSK inhibitory potency, elimination of C^7 chirality does not appear to impact RSK inhibitory potency, removal of the N^5-substitution is required for potent RSK inhibition. We have identified compounds that inhibit RSK2 activity in cells and our cellular viability and toxicity studies suggest that RSK2 inhibition is uncoupled from potent cytotoxicity in AML cells. Our studies have provided important structural information for the development of pteridinone-based RSK inhibitors and potential insights into structural modifications that may limit metabolism and improve RSK selectivity.

2. Results and Discussion

2.1 Computational-based RSK2 inhibitor design

Although the NTKD crystal structures for both RSK1 and RSK2 have been resolved, we utilized the RSK2 NTKD structure co-crystallized with BI-D1870 for our computational-based docking simulations and inhibitor design studies,[28] as we could directly compare the *in silico* predicted binding with the co-crystallized conformation of BI-D1870. The RSKs share a high degree of homology, particularly in the ATP-binding site, and the objective of this study was to understand the structural properties required for RSK inhibition and not to examine the potential for isoform selectivity; therefore, the crystal structure of the NTKD of RSK2 was used for all computational-based docking simulations. The preparation of the BI-D1870 structure for docking simulations highlighted the chiral carbon at C^7, an often-overlooked feature of BI-D1870. Interestingly, while the *R*-isomer is the species co-crystallized with RSK2, the modeling results suggested that both isomers of BI-D1870 are capable of binding to RSK2. Overall, our docked conformation for BI-D1870 was similar to that of the RSK2 co-crystallized BI-D1870 structure and displayed few binding interactions with the residues of the ATP-binding site of the RSK2 NTKD (**Figure 2**), which is surprising for a potent, nanomolar inhibitor. As is common to many ATP-competitive kinase inhibitors, the modeling revealed a donor-acceptor motif of H-bond interactions present between the core pteridinone heterocycle of BI-D1870 and the kinase hinge backbone residues Asp148 and Leu150. An additional H-bond interaction also occurs between the phenol of BI-D1870 and the carbonyl of Asp211in the DFG motif.

To confirm the necessity of the H-bond interaction with DFG motif, we synthesized negative control compounds that either lack the hydroxyl group (**24**) or substitute it for a methoxy group (**25**). In addition, we examined whether a carbon extension of the phenol to a benzyl alcohol could extend the position of the H-bond donor further into the binding pocket and offer an improved bond angle and orientation for the interaction to occur. A means for synthesizing the difluoro-benzyl alcohol building block required for this compound was not readily commercially available, requiring alternative synthesis of the benzylic alcohol lacking the fluorine atoms (**26**) to test this modification. In order to account for more than one modification, the unsubstituted phenol analog of BI-D1870 (**27**) was also proposed to allow for direct comparison. The fluorine atoms present in BI-D1870 likely serve to protect the compound from ortho- oxidative metabolism of the phenol ring; however, the substitution pattern and identity of the halogen atoms, and hence their electronic effects may also serve to optimize the pKa of the phenol hydrogen to facilitate H-bonding with Asp211 of the DFG motif. Therefore, both the mono- and di-halogenated analogs containing fluorine, chlorine, and bromine were proposed (**28-32**) in order to identify the ideal substitution pattern and electron-withdrawing characteristics adorning the phenol ring to facilitate this key H-bond interaction. The docked conformation of BI-D1870 in the ATP-binding site of the RSK2

NTK [illegible] n of not make any key interactions with the kinase other than hydrophobic contacts (**Figure 2**). Therefore, we proposed to remove the piperazinone ring and sequentially add functional complexity present in the parent compound to the pyrimidine core (**38**), to determine the structural components required for binding of BI-D1870 to RSK2. The compounds proposed included the aminonitropyrimidine pseudocycle (**43**), the diaminopyrimidine (**44**), and the pteridines lacking the N^5-methyl (**33**), lacking the N^8-isopentyl chain (**39**), and devoid of C^7 chirality (**34**).

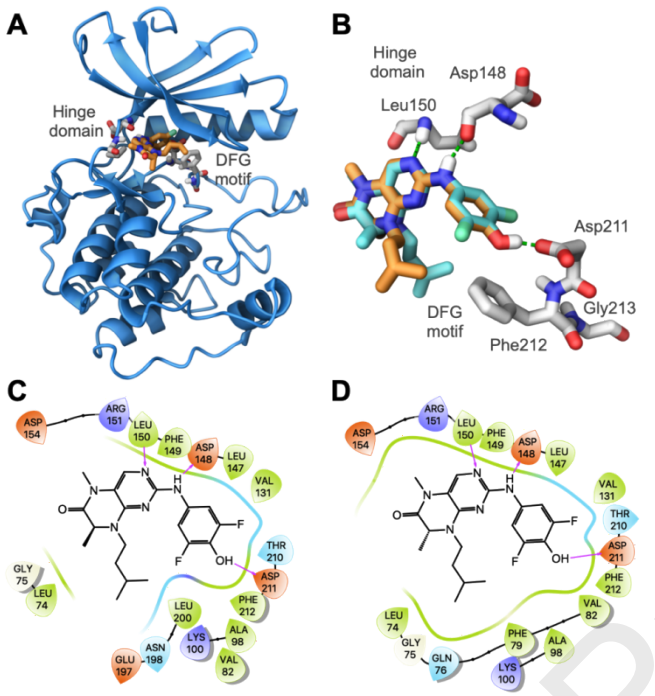

Figure 2. Crystal structure of the NTKD of RSK2 (PDB: 5D9K) with docked BI-D1870. **(A)** Ribbon representation of the RSK2 NTKD with amino acid residues of the hinge domain and the DFG motif displayed in stick form (grey) with the docked *R*-isomer of BI-D1870 (orange). **(B)** Stick display style representation of the docked conformation of the *S*-isomer (cyan) and *R*-isomer (orange) of BI-D1870 and key interacting amino acid residues (grey), where green dashed lines indicate H-bonds. Ligand interaction map of the predicted binding mode of **(C)** the *S*-isomer and **(D)** the *R*-isomer of BI-D1870 in the ATP-binding site of the RSK2 NTKD, where red residues are charged negative, purple residues are charged positive, green residues are hydrophobic, and blue residues are polar, and purple arrows indicate H-bonds.

2.2 Chemical synthesis of BI-D1870 analogs

A series of 19 analogs of BI-D1870 were synthesized in order to investigate the structural components of BI-D1870 necessary for potent RSK inhibition. In general, various anilines were coupled to the heterocyclic core of BI-D1870 or analogs thereof using a trifluoroacetic acid (TFA) and trifluoroethanol (TFE)-mediated S_NAr reaction according to Carbain *et al.*[29] To synthesize the pteridinone heterocyclic core of BI-D1870 (**Scheme 1**), 1-bromo-3-methylbutane (**4**) was coupled with benzylamine (**5**) to afford the desired secondary amine (**6**), which was subsequently reacted with ethyl 2-bromopropanoate to generate intermediate **7**. To synthesize the analogous intermediate lacking a chiral carbon (**10**), a reductive amination between isovaleraldehyde (**8**) and benzylglycine ethyl ester (**9**) was performed in the presence of sodium cyanoborohydride. The benzyl protecting groups of intermediates **7** and **10** were removed *via* a palladium-mediated amino acid ethyl esters **11** and **12**. These, along with alanine ethyl ester (**13**), were reacted with 2,4-dichloro-5-nitropyrimidine (**14**) to generate the required 4-amino-5-nitropyrimidines, both containing (**15-16**) and lacking (**17**) the N^8-isopentyl group present in BI-D1870. An iron/acetic acid reduction of the 5-nitro group with concomitant pteridinone cyclization was utilized to form the heterocyclic intermediates **18**, **19**, and **20**, which were subsequently methylated at the N^5-position to generate the core pteridinones **21**, **22**, and **23**.

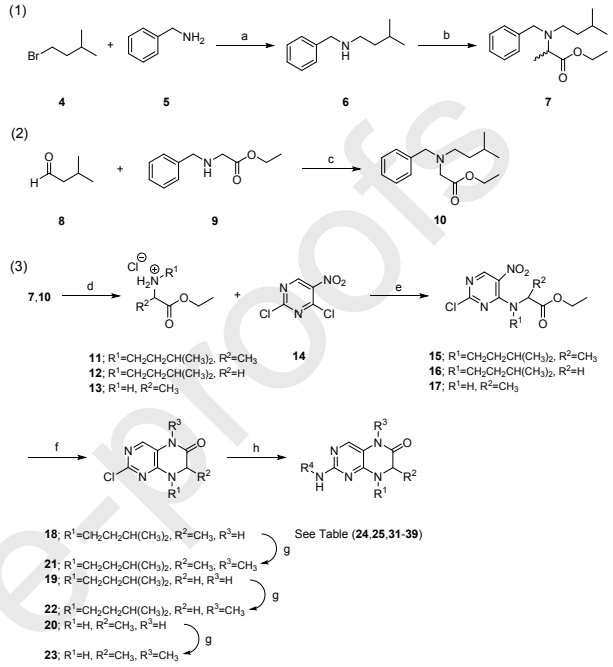

Scheme 1. Synthesis substituted pteridinones. Reagents and conditions: (a) Cs_2CO_3, DMF, rt, 48 h; (b) ethyl 2-bromopropionate, K_2CO_3, DMF, 110°C, 4 h; (c) i) MeOH, 10% AcOH, 50°C, 1 h; ii) $NaBH_3CN$, 50°C, 1 h; (d) 10% Pd/C, H_2, EtOH, 10M HCl, rt, 2-16 h; (e) Et_2O/H_2O, K_2CO_3, -15°C, 2 h; (f) Fe, AcOH, 70°C → 100°C; (g) MeI, NaH, DMA, -15°C, 30 min; (h) relevant aniline, TFA, TFE, MW, 140°C, 30 min.

While the dichlorino aniline was commercially available, the difluoro- (**41**) and dibromoanilines (**42**) were generated from the dihalonitrophenols using a tin(II) chloride nitro reduction. The N^5-unmethylated (**18-20**) and methylated (**21-23**) pteridinone cores were then coupled in combination with the corresponding aniline to generate final compounds **24**, **25**, and **31-39** (**Scheme 1**). In following the TFA/TFE-mediated synthetic approach, the proposed compounds investigating carbon extension of the phenol underwent coupling *via* nucleophilic attack by both the aniline and the phenol, and thus an alternative approach was required. 4-Nitrophenol and 4-nitrobenzyl alcohol were alternatively protected at the hydroxyl position with triisopropylsilylchloride, reduced to the corresponding aniline, and coupled to the pteridinone core **21** *via* a Buchwald-Hartwig amination. Successive TIPS-deprotection was performed to generate compounds **26** and **27** (**Supplemental Scheme S1**). In investigating a means for the most efficient synthetic route for generating BI-D1870 analogs, all mono-halogenated anilines were prepared from the corresponding methoxy-pteridinone intermediates via TFA/TFE coupling and subsequent BBr_3 demethylation to yield compounds **28-30** (**Supplemental Scheme S2**). These compounds collectively investigate how amendable BI-D1870 is to modification of the halogen substitution pattern, removal of the N^5-methyl, removal of the N^8-isopentyl chain, and

elim
domain of RSK2. Finally, to examine modification to the pteridinone core of BI-D1870, 2,4-dicholoro-5-nitropyrimidine was treated with ammonia to selectively displace the 4-chloro atom and yield intermediate **40** (**Scheme 2**). Difluoroaniline **41** was then coupled to afford aminonitropyrimidine pseudocycle **43**, the 5-nitro group of which was reduced with tin(II) chloride to give the 4,5-diaminopyrimidine **44**.

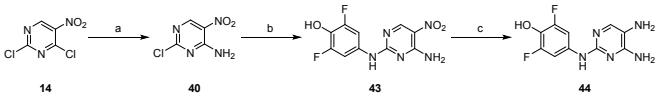

Scheme 2. Synthesis substituted pyrimidines. Reagents and conditions: (a) 2M NH_3/EtOH, DCM, 0°C → RT, 45 min; (b) aniline **43**, TFA, TFE, MW, 140°C, 30 min; (c) $SnCl_2$, EtOH, reflux, 24 h.

2.3 Inhibition of RSK2 kinase activity

The synthesized compounds were tested in a recombinant TR-FRET kinase inhibition assay against RSK2 and their half-maximal inhibitory potency values (IC_{50}) were calculated using nonlinear regression analysis of the log dose-response (**Table 1, Table 2**). Compounds found to have either improved or equipotent activity when compared to BI-D1870 (RSK2 IC_{50} = 23.3 ± 8.2 nM) were tested against the remaining three RSK isoforms (**Supplemental Table S1**) to probe for isoform selectivity and were selected for cellular testing. As anticipated, elimination of the H-bond interaction between the kinase DFG-motif and the phenol of BI-D1870 with **24** and **25** led to a complete loss in potency, demonstrating the necessity of this interaction for RSK inhibition. While the carbon extension of the phenol to the benzyl alcohol caused a significant loss in potency, this may be attributed to the loss of the two fluorine atoms, as a decrease in activity was likewise observed for the accompanying unsubstituted phenol. The two fluorine atoms of BI-D1870 may play a role in improving metabolic stability, but also alter the pKa of the adjacent phenol and, consequently, the ability of the phenol to H-bond with Asp211 of the DFG motif. The stepwise improvement in inhibitory activity between monobromo **30**, monochloro **29**, and monofluoro **28** analogs may be attributed to the electronic effects of the halogen substitutions, and thus, the pKa of the phenol. However, it is also possible that the steric bulk of the chlorine and bromine substituents may not be well tolerated in comparison to smaller hydrogen and fluorine atoms, as indicated by the improved activity of the unsubstituted phenol in comparison to **29** and **30**. Complete loss of activity occurred with both the dichloro **31** and dibromo **32** analogs and is further indication that the steric bulk and/or electronic effects of chloro- and bromo-substitutions are sub-optimal for RSK2 inhibition.

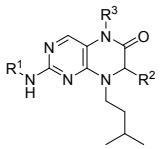

Compound	R^1	R^2	R^3	RSK2 Inhibition
BI-D1870 (**1**)		CH_3	CH_3	23.3 ± 8.2 nM
24		CH_3	CH_3	71% @ 10 μM
25		CH_3	CH_3	43% @ 10 μM
26		CH_3	CH_3	739 ± 14.1 nM
27		CH_3	CH_3	54.8 ± 1.4 nM
28		CH_3	CH_3	25.4 ± 3.2 nM
29		CH_3	CH_3	71.5 ± 10.3 nM
30		CH_3	CH_3	141 ± 25.7 nM
31		CH_3	CH_3	83% @ 10 μM
32		CH_3	CH_3	78% @ 10 μM
33		CH_3	H	18.2 ± 1.4 nM
34		H	CH_3	17.6 ± 1.4 nM
35		H	H	38.3 ± 7.9 nM
36		H	H	23.4 ± 4.7 nM
37		H	CH_3	24.7 ± 1.8 nM

Table 1. Inhibition of RSK2 activity by substituted pteridinones. Inhibitory activity of compounds in the TR-FRET kinase assay against RSK2 given as the half-maximal inhibitory concentrations (IC_{50}) or percentage inhibition; values are the mean ± S.D. (n=3).

As presented in **Table 2**, replacement of the pterdinone core of BI-D1870 with a pyrimidine resulted in complete loss of activity. In addition, all the compounds that sequentially incorporated components of the core pteridinone heterocycle resulted in reduced RSK2 inhibitory activity. Interestingly, removal of the N^8-isopentyl chain alone caused a complete loss in activity against RSK2. Removal of the N^5-methyl group of BI-D1870 was not only advantageous as a means to reduce the number of synthetic steps, it also offered some improvement in activity over BI-D1870. Additionally, eliminating chirality is attractive in order to avoid enantiomer selectivity potentially attenuating the activity of the racemate, and removal of the chiral C^7 also improved inhibitory potency. After analyzing the initial TR-FRET results, several additional compounds were synthesized combining modifications

that respect to BI-D1870 (**35-37**). These include monofluoro halogenation of the phenol ring, removal of the N^5-methyl from the pteridinone, and elimination of C^7-chirality. Interestingly, combinations of these modifications did not result in any substantial additive improvements in RSK2 inhibitory potency as all three analogs demonstrated equivalent RSK2 inhibitory activity as BI-D1870. For comparison, the previously described compounds LJH685 and LJI308 were also tested against RSK2 activity and resulted in improved inhibitory potency over BI-D1870 (LJH685 IC_{50} = 11.8 ± 0.5 nM; LJI308 IC_{50} = 12.9 ± 0.3 nM, **Supplemental Table S2**), which is in agreement with published literature.[28]

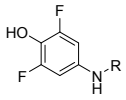

Compound	R	RSK2 Inhibition
38		45% @ 10 µM
39	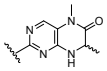	83% @ 10 µM
43		72% @ 10 µM
44		38% @ 10 µM

Table 2. Inhibition of RSK2 activity by substituted pyrimidines. Inhibitory activity of synthesized compounds in the TF-FRET kinase assay against RSK2 given as percentage inhibition; values are the mean (n=3).

2.4 Growth inhibition and cytotoxic effects of RSK2 inhibitors

The compounds that exhibited activity in the kinase activity assay within the concentration range of BI-D1870 were evaluated in cell systems for effects on cell viability and toxicity. A series of leukemic cell lines were analyzed for constitutive phospho- and total-RSK1 and RSK2 protein via Western Blot (**Supplemental Figure S1**) to ensure use of an appropriate cell line for these assays. From these data, it was determined that MOLM-13 cells expressed robust quantities of active RSK1 and RSK2 and these cells were used for all cell viability and cytotoxicity assays. Results from an MTS assay offered initial insights into the effects of inhibitors on cellular viability (**Figure 3A**). After treatment with inhibitors for 72 h, the mono-fluoro analog **28** was the only compound to demonstrate improved inhibition of cell growth over BI-D1870, while the pteridinone lacking C^7-chirality (**34**) displayed equipotency to BI-D1870. Despite analog **34** showing no improvement in activity in this assay, eliminating chirality while retaining effects on cell viability may be a key finding for further development of the BI-D1870 molecule. Interestingly, pteridinone **33** lacking the N^5-methyl and the known RSK inhibitors LJH685 and LJI308 demonstrated minimal effects on cell viability despite being potent RSK2 inhibitors.

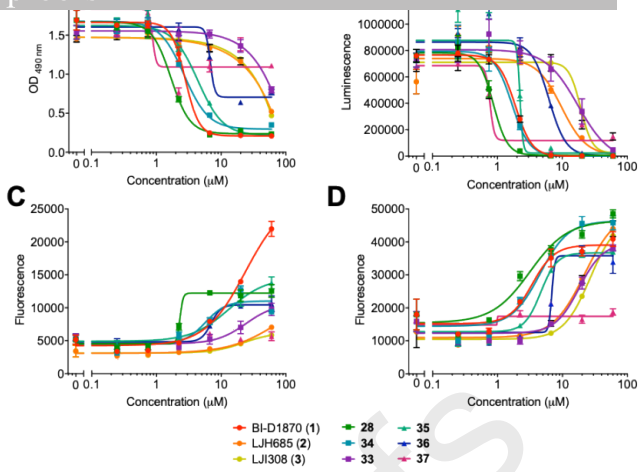

Figure 3. Cellular effects of RSK inhibitors on viability and toxicity in MOLM-13 cells. Dose-response curves for RSK inhibitors treated over a concentration range from 60 µM to 250 nM in an MTS assay **(A)** and CellTiter-Glo assay **(B)** after 72 h. Dose-response curves for RSK inhibitors treated for 24 h **(C)** and 72 h **(D)** over a concentration range from 60 µM to 250 nM in a CellTox Green assay (n = 3, error bars: ± S.D.).

To gain further insight into the potential mechanism of action of RSK inhibitors, a CellTiter-Glo® cell viability assay (**Figure 3B**) and a CellTox™ Green cellular toxicity assay (**Figure 3C, Figure 3D**) were performed in MOLM-13 cells. The results suggest that BI-D1870 and potent analogs thereof act as cytotoxic agents rather than cytostatic, as indicated by the equivalent and potent EC_{50} values determined for BI-D1870 in the viability and toxicity assays after 72 h. Results in the CellTiter-Glo® assay for all synthesized analogs coincide with the trends seen in the MTS assay in which compound **28** was the only analog to demonstrate improved potency over BI-D1870. Again, compound **34** displayed equipotency to BI-D1870 and **33**, LJH685 and LJI308 exhibited significantly diminished effects on MOLM-13 cell viability. Additional evidence to suggest that BI-D1870 and its inhibitory analogs act in a cytotoxic manner was the dramatic increase in cellular toxicity at 72 h. Interestingly, BI-D1870 was the only cytotoxic compound at 24 h, but all compounds exhibited cytotoxicity after 72 h, with analogs **28**, **34**, and **35** demonstrating equipotent cytotoxic effects to BI-D1870, while **33**, LJH685, and LJI308 exhibited some cytotoxicity but to a lesser degree than BI-D1870 (**Table 3**).

Compound	MTS 72 h EC_{50} (µM)	CellTiter-Glo 72 h EC_{50} (µM)	CellTox Green 72 h EC_{50} (µM)
BI-D1870 (**1**)	2.80 ± 0.17	1.89 ± 0.04	3.41 ± 0.53
LJH685 (**2**)	75% @ 60 µM	9.71 ± 0.75	22.0 ± 5.08
LJI308 (**3**)	79% @ 60 µM	19.1 ± 0.48	23.38 ± 3.22
28	1.69 ± 0.24	0.87 ± 0.04	3.16 ± 0.51
33	56% @ 60 µM	17.4 ± 3.5	18.1 ± 2.55
34	2.71 ± 0.10	1.67 ± 0.11	4.54 ± 0.40
35	4.39 ± 0.28	2.23 ± 0.06	4.64 ± 0.10
36	6.82 ± 0.12	6.20 ± 0.26	6.85 ± 0.15

Table 3. Cellular effects of RSK inhibitors on viability and toxicity in MOLM-13 cells. Inhibitory activity of compounds in the TR-FRET kinase assay against RSK2 as the half-maximal inhibitory concentrations (IC_{50}) values are the mean ± S.D. (n=3). EC_{50} values or percentage inhibition values from cellular assays were determined for RSK inhibitors treated for over a concentration range from 60 µM to 250 nM.

Inhibitors of purified RSK2 activity identified in the TR-FRET assay were evaluated for their capacity to inhibit intracellular RSK2 using a NanoBRET™ intracellular kinase assay (**Figure 4, Supplemental Figure S2**). Compound **28** had no direct effect on cellular RSK2 activity compared with BI-D1870, despite being the only analog to show an improvement in inhibitory potency over BI-D1870 against MOLM-13 cellular viability and toxicity. Conversely, **33**, LJH685, and LJI308 had a minimal impact on cell viability and toxicity but were the only compounds to demonstrate inhibition of cellular RSK2 activity, albeit at a lower potency than that of BI-D1870. Collectively, the data from the cell-based experiments suggest that the effects and impact on cellular viability and toxicity seen with BI-D1870 and the synthesized RSK inhibitors are independent of their effects on cellular RSK2 inhibition alone and most likely result of interactions with both RSK2 and alternative molecular targets. Collectively, the data support that cellular RSK2 inhibition is possible with compound **33**, LJH685, and LJI308 without potent and acute cytotoxic effects.

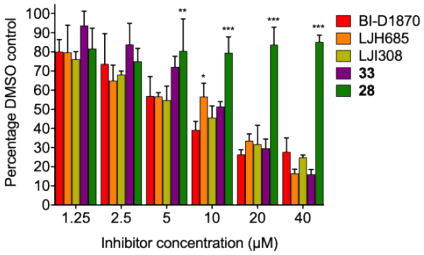

Figure 4. Inhibition of cellular RSK2 activity measured by nanoBRET assay. Representative BRET ratio compared to DMSO control. Inhibitors were treated over a concentration range of 40 μM to 1.25μM for 2 h (n = 3, error bars: ± S.D.). Each compound was analyzed in relation to BI-D1870 $*P < 0.05$; $**P < 0.005$; $***P < 0.0001$, two-way ANOVA.

We have developed a series of substituted pteridinones and pyrimidines to examine the structural features of BI-D1870 that are required for potent inhibition of RSK2 kinase activity. The *S*- and *R*-isomers of BI-D1870 were docked into the ATP-binding site of the RSK2 NTKD crystal structure to guide the design of BI-D1870 analogs. Overall, the BI-D1870 *R*- and *S*-isomers had similar docked conformations and interactions with residues in the hinge domain and DFG motif. We designed compounds to replace the substituents of BI-D1870 that displayed interactions with the DFG motif and those that did not appear to interact with amino acid residues in the ATP-binding site. Our studies revealed that the H-bond interaction between the phenol and Asp211 was critical for RSK2 inhibition, the halogen substitution of the phenol has a significant impact on binding affinity, removal of the N^5 methyl maintains RSK2 inhibitory potency, but removal of the N^8-isopentyl or the piperazinone ring abolished RSK2 inhibitory activity. The chiral C^7 of BI-D1870 has been an overlooked feature of this commonly used pan-RSK inhibitor and the removal of the chiral center in compound **34** demonstrated some modest improvement in RSK2 inhibition in the TR-FRET assay. However, in the nanoBRET assay, inhibition of cellular RSK2 activity was observed with only BI-D1870, LJH685, LJI308, and **33**, and to a lesser extent with **35** and **36**, but no appreciable inhibition was achieved with **34** or **37**. This reduction in RSK2 inhibitory potency for **34-37** in cells may be due to interaction with other cellular targets as supported by the cell viability and cytotoxicity data. The compounds **28**, **34**, and **37** demonstrated potent effects on cell cytotoxicity after 72 h of exposure.

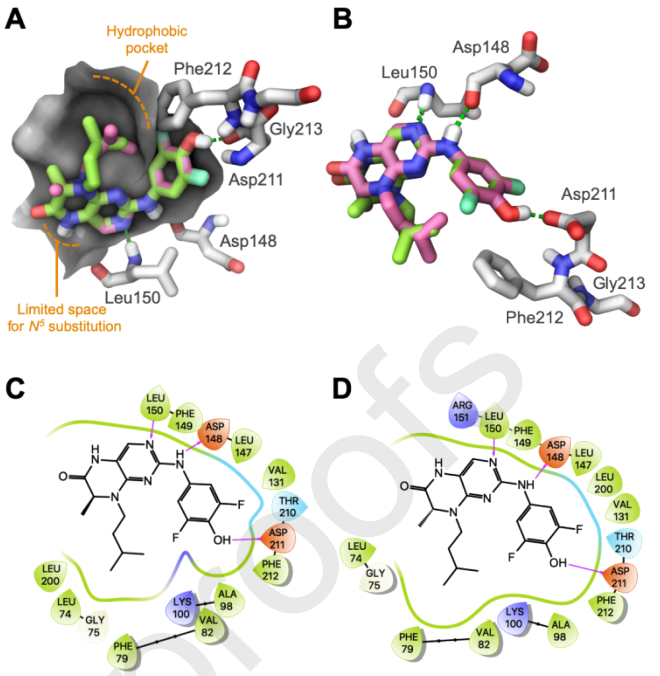

Figure 5. Compound **33** docked into the crystal structure of the NTKD of RSK2 (PDB: 5D9K). **(A)** Molecular surface of the ATP-binding site (colored grey) displaying the hydrophobic pocket between the Phe79 and Val82 residues and the limited scope for N^5 modification with the docked *S*-isomer (green) and *R*-isomer (pink) of compound **33**. **(B)** Stick display style representation of the docked conformation of the *S*-isomer (green) and *R*-isomer (pink) of compound **33** and key interacting amino acid residues (grey), where green dashed lines indicate H-bonds. Ligand interaction map of the predicted binding mode of **(C)** the *S*-isomer and **(D)** the *R*-isomer of **33** in the ATP-binding site of the RSK2 NTKD, where red residues are charged negative, purple residues are charged positive, green residues are hydrophobic, and blue residues are polar, and purple arrows indicate H-bonds.

Interestingly, we are the first to report inhibition of cellular RSK2 activity using the known RSK inhibitors BI-D1870, LJH685, and LJI308 in the nanoBRET intracellular kinase assay. In fact, no cellular engagement assessment of LJH685 and LJI308 has previously been reported. The determination of direct inhibition of cellular RSK activity by small molecules by ELISA or Western blot can be confounding due to the numerous RSK substrates that can be activated by other kinases.[30] Overall, LJH685, LJI308, and **33** demonstrated potent inhibition of cellular RSK2 activity, but did not display potent effects on cell viability or acute cytotoxicity, with cytotoxic effects only observed in MOLM-13 cells at high concentrations after 72 h of exposure. Although BI-D1870 is a potent pan-RSK inhibitor and has narrow-spectrum kinome activity, some non-specific interactions have been reported, and combinations of these interactions may contribute to its potent inhibition of cell growth and induction of cytotoxicity. BI-D1870 was originally developed in a campaign to identify PLK1 inhibitors and it is a nanomolar inhibitor of PLK1, but a more potent inhibitor of the RSKs.[22, 24] Therefore, the combination of RSK and PLK1 inhibition could contribute to the potent cytotoxicity observed in MOLM-13 cells. Additionally, BI-D1870 may also interact with proteins outside of the kinome and it has been reported to interact with the bromodomain (BRD) containing bromo and extra terminal (BET) BRD4 protein with a K_d of 3.5 ±

of BI-D1870 for BRD4 compared with the dihydropteridinone BI-D2536 was proposed to be due to the methyl group at C^7 reducing hydrophobic contact with the BRD compared with the ethyl group of BI-D2536. Therefore, in the case of compound **33** the methyl group at C^7 and the lack of methyl substitution of N^5 not only reduces hydrophobic contact but also alters the acetyl-lysine mimetic group required for BRD binding which could explain its reduced cytotoxicity. However, compounds **35** and **36** are unsubstituted at C^7 and N^5 further reducing the potential for hydrophobic contact wih BRD4 and altering the acetyl-lysine mimetic group, but these compounds demonstrated potent cytotoxicity in MOLM-13 cells. Collectively, these data suggest that the potent cytotoxicity of compounds **35** and **36** was not a direct result of interacting with BRD4 or there is an alternative SAR for BRD binding. Our SAR study supports that N^5 substitution is not required for RSK inhibition as demonstrated with compounds **33**, **35**, and **36**; however, the most potent RSK2 inhibition was recorded for **33** without the potent cytotoxicity observed with **35** and **36**. The docking of compound **33** to RSK2 reveals that removal of the N^5 methyl does not result in additional interactions or alter the interactions with the hinge domain residues or the DFG motif observed for BI-D1870 and comparing the docked conformations of the two compounds there is limited space to accommodate N^5 substitutions (**Figure 5**). Overall, the data from our study indicate that the SAR for RSK inhibition without potent cytotoxicity is narrow for pteridinone analogs of BI-D1870.

The primary goal of our study was to identify the structural components of BI-D1870 that were required for RSK2 inhibition and those that were amenable to modification to further support the development of pteridinone-based RSK2 inhibitors (**Figure 6**). Our study confirmed that the phenol H-bond with Asp211 of the DFG motif was a critical interaction for RSK2 inhibition, but this moiety may be prone to metabolism and protective prodrug strategies may be necessary. The development of a prodrug of a RSK2 inhibitor may be an interesting strategy as it would be more feasible to develop a tumor-selective prodrug than an RSK-isoform selective inhibitor. Furthermore, prodrug forms of RSK inhibitors may facilitate the accumulation of RSK inhibitors in the cell and, thus, prolonged RSK inhibition. Another important result from our SAR study was that the removal of the N^8-isopentyl chain from the pteridinone ring of BI-D1870 abolished RSK2 inhibitory activity (**Table 2**). From our computational models of the BI-D1870 isomers docked into RSK2 and the co-crystal structures of RSK2 with BI-D1870 or LJH685,[27, 28] the isopentyl of BI-D1870 and phenylpiperazinyl of LJH685 extend out of the ATP-binding site and into a hydrophobic pocket towards the kinase substrate binding site. The extension and optimization of substituents from the N^8 of the pteridinone ring into this hydrophobic region may present the opportunity for improvement in inhibitory potency and potentially RSK isoform selectivity.

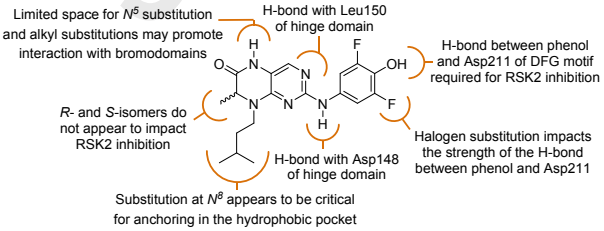

Figure 6. General pteridinone pharmacophore model for RSK inhibition.

In summary, we demonstrate that prolonged exposure of cells to high concentrations of RSK inhibitors LJH685, LJI308, and **33** was required to induce cytotoxicity in MOLM-13 cells. This finding was surprising as the RSKs phosphorylate a number of substrates involved in many diverse cellular processes critical for cell survival. It is possible that some cell types may be more sensitive to RSK inhibition; however, the MOLM-13 cells were selected from a panel of leukemic cancers as it had high levels of activated RSK1 and RSK2 (**Supplemental Figure S1**), supporting that RSK1 and RSK2 are mediating functions in the cell. Therefore, the N^5 unsubstituted compound **33** may be a more selective RSK inhibitor than BI-D1870, as it has equivalent RSK2 inhibitory potency, but has dramatically reduced cytotoxicity and mirrors more the overall profiles for LJH685 and LJI308. Further studies are required to determine the impact of RSK inhibition in cancer cells as synergistic combination therapies may need to be identified,[32] or RSK inhibitors may be therapeutically more effective in a different context, such as eliminating the cancer stem cell population.[33] Our findings indicate there is still further scope for the development of novel RSK inhibitors and that RSK inhibition alone is not sufficient to induce acute cytotoxicity in MOLM-13 cells.

4. Experimental

4.1 Computational-based modeling

The pteridinones and pyrimidines were docked into the ATP-binding site of the NTKD of RSK2 (PDB: 5D9K) crystal structure,[28] using the Glide module within Schrödinger (Release 2018-1, Schrödinger LLC, New York, NY).[34-36] The compounds were prepared using LigPrep by generating possible states at the target pH 7 .0 using Epik and minimized by applying the OPLS_2005 force field.[37] The crystal structure of the NTKD of RSK2 co-crystallized with BI-D1870 (PDB: 5D9K) was obtained from the Protein Data Bank (PDB) [28]. The water molecules were removed from the RSK2 structure and the protein was prepared by assigning bond orders, adding hydrogens, and repairing any side chains or missing amino acid sequences. To complete protein preparation a restrained minimization of the RSK2 structure was performed using the default constraint of 0.30Å RMSD and the OPLS_2005 force field.[37] The prepared proteins were subjected to SiteMap analysis,[36] that identified the ATP-binding site in the NTKD and docking grids were generated using Receptor Grid Generation. Molecular docking simulations were performed using the Glide ligand docking module in XP (extra precision) mode and included post-docking minimization.[35] The docked structures of BI-D1870 in the ATP-binding site of the RSK NTKD were used as the basis for the design of the pteridinones and pyrimidines, with the aim of examining substitutions to test the importance of interactions with residues in the ATP-binding site. The pteridinones and pyrimidines were prepared and docked in the RSK2 crystal structure in order to identify the critical interactions that resulted in RSK inhibition.

4.2 Chemistry

All melting points (M.p.) were determined using a Mettler Toledo M540 melting point apparatus. ^{1}H and ^{13}C nuclear magnetic resonance (NMR) spectra were obtained as solutions in deuterated solvents DMSO-d_6 or $CDCl_3$ using a 400 MHz Bruker Avance III 400 spectrometer. Chemical shifts (δ) are reported in parts per million (ppm) and the spin-multiplicity abbreviated as: s (singlet), d (doublet), t (triplet), q (quartet), quin (quintet), m (multiplet), bs

(bro... with coupling constants (*J*) given in Hertz (Hz).High-resolution mass spectrometry (HRMS) was performed using an Agilent 6520 tandem quadrupole-time of flight (Q-TOF) mass spectrometer coupled to an electrospray ionization source. Spray was induced with a capillary voltage of 4000V and the fragmentor voltage was 200V. Data was acquired over a range of m/z 50-1700. Compound purity was determined by NMR and mass spectrometry analysis. Fourier Transform Infrared (FTIR) spectra were obtained using a Bruker Alpha Platinum-ATR as a neat sample.

General Procedure A. A solution of benzyl-protected amino acid ethyl ester (**7, 10)** (1 equiv.) and Pd/C (10% w/w) in EtOH (0.3M) containing concentrated HCl (10M) was hydrogenated for 2 h prior to filtration of the catalyst. The material was concentrated *in vacuo* to afford the desired compound.[38]

General Procedure B. A solution of the amino acid ethyl ester precursor (**11-13**) (1.2 equiv.) in H_2O (0.6M) was added to a stirring solution of 2,4-dichloro-5-nitropyrimidine (1 equiv.) in Et_2O (0.25M). The reaction was cooled to -15°C and K_2CO_3 (4.8 equiv.) was added slowly before the reaction was warmed to RT over 2 h. The phases were partitioned and the organic phase was extracted with Et_2O (3 x 10 mL/mmol) and the combined organic extracts were dried ($MgSO_4$), concentrated *in vacuo*, and purified *via* gel chromatography, if necessary, to afford the desired compound. [38]

General Procedure C. A solution of the necessary nitropyrimidine (**15-17**) (1 equiv.) in acetic acid (0.2M) was heated to 70°C prior to the addition of iron powder (5 equiv.). The solution was further heated to 100°C, stirred for 30 minutes, and filtered hot. The filtrate was concentrated *in vacuo* before being partitioned between EtOAc (20 mL/mmol) and a saturated $NaHCO_3$ solution (20 mL/mmol) and extracted with EtOAc (3 x 15 mL/mmol). The combined organic extracts were dried ($MgSO_4$) and concentrated *in vacuo*, and the crude residue was purified *via* silica gel chromatography to afford the desired compound.[38]

General Procedure D. To an oven dried flask cooled under N_2 was added a solution of pteridinone **18-20** (1 equiv.) in DMA (0.37M). The solution was cooled to -15°C and NaH (1.1 equiv., 60% dispersion in mineral oil) was added followed by subsequent addition of MeI (1.2-4.0 equiv.). The solution was stirred for 30 minutes before being quenched dropwise onto ice. The organic material was extracted with EtOAc (3 x 10 mL/mmol), the combined organic extracts were dried ($MgSO_4$), and concentrated *in vacuo*. The resultant residue was purified *via* column chromatography, if necessary, to afford the desired compound.[38]

General Procedure E. The relevant halogenated heterocycle (1.0 equiv.), substituted aniline (2.0 equiv.) and TFA (5.0 equiv.) were taken up in TFE (0.1M) and heated under microwave irradiation conditions at 140°C for 30 minutes before being concentrated *in vacuo*. The residue was resuspended in EtOAc:THF (1:1, 20 mL/mmol), washed with saturated $NaHCO_3$ solution (20 mL/mmol), and the aqueous phase was further extracted with EtOAc:THF (1:1, 3 x 15 mL/mmol). The combined organic extracts were washed with brine, dried ($MgSO_4$) and concentrated *in vacuo*. The resultant residue was purified *via* column chromatography and/or triturated as specified to afford the desired compound.[29]

General Procedure F. To an oven dried flask cooled under N_2 was added a solution of methoxyanilino pteridinone **(51-53)** (1 equiv.) in DCM (0.2M). The solution was cooled to 0°C before a solution was held at 0°C for 30 minutes then allowed to warm to RT and stirred for an additional 2.5 h. The reaction was quenched *via* dropwise addition onto ice water (50 mL/mmol) before being washed with saturated $NaHCO_3$ solution (20 mL/mmol) and extracted with EtOAc:THF (1:1, 3 x 15 mL/mmol). The combined organic extracts were washed with brine, dried ($MgSO_4$) and concentrated *in vacuo*. The crude residue was purified *via* silica gel chromatography to give the desired compound.

4.2.1 N-Benzyl-3-methylbutan-1-amine (6). A solution of cesium carbonate (0.43 g, 1.32 mmol) and benzyl amine (**5**) (290 µL, 2.65 mmol) in DMF (4.5 mL, 0.29 M) was stirred at RT for 30 min prior to the addition of alkyl halide **4** (159 µL, 1.32 mmol). The reaction was stirred for 48 h before the solid material was removed via filtration and washed with EtOAc (20 mL). The organic filtrate was then washed thoroughly with H_2O (6 x 30 mL) and the combined organic extracts were washed with brine (30 mL), dried ($MgSO_4$), and concentrated *in vacuo.*[38] The crude residue was purified *via* silica gel chromatography (19:1 DCM:MeOH) to afford the desired compound as a yellow oil (3.83 g, 21.6 mmol, 73%). Rf 0.24 (19:1 DCM:MeOH); IR (cm^{-1}) 3061, 3027, 2953, 2918, 2868, 2814, 1675, 1604, 1547; ^{1}H NMR (400 MHz, DMSO-d_6) 0.84 (6H, d, J = 6.7 Hz, $CH(CH_3)_2$), 1.31 (2H, dt, J = 7.4, 7.1 Hz, $NHCH_2CH_2$), 1.51-1.69 (1H, m, $CH(CH_3)_2$), 1.97 (1H, bs, NH), 2.47 (2H, t, J = 7.4 Hz, $NHCH_2CH_2$), 3.67 (2H, s, benzyl CH_2), 7.16-7.25 (1H, m, H-4), 7.25-7.40 (4H, m, H-2/3/5/6); ^{13}C NMR (100 MHz, DMSO-d_6) 23.1 ($CH(CH_3)_2$), 26.0 ($CH(CH_3)_2$), 47.3 ($NHCH_2CH_2$), 53.6 (benzyl CH_2), 126.9 (Ar-C), 128.3 (Ar-C), 128.5 (Ar-C), 141.6 (Ar-C).

4.2.2 Ethyl N-benzyl-N-isopentylalaninate (**7**). A solution of amine **6** (52 mg, 0.28 mmol), ethyl 2-bromopropionate (37 µL, 0.28 mmol), and K_2CO_3 (61 mg, 0.42 mmol) taken up in DMF (0.35 mL, 0.8M) was heated to 110°C and stirred for 4 h prior to filtration of the inorganic salts. The filtrate was concentrated *in vacuo*, resuspended in diethyl ether (15 mL), washed with H_2O (10 mL) and extracted with ether (3 x 15 mL).[38] The combined organic extracts were dried ($MgSO_4$) and concentrated *in vacuo* to afford the desired compound as a yellow oil (3.12 g, 11.2 mmol, 74%). Rf 0.81 (19:1 DCM:MeOH); IR (cm^{-1}) 3061, 3028, 2954, 2867, 1728; ^{1}H NMR (400 MHz, DMSO-d_6) 0.75 (3H, d, J = 6.7 Hz, $CH(CH_3)_2$), 0.77 (3H, d, J = 6.7 Hz, $CH(CH_3)_2$), 1.19 (3H, d, J = 7.1 Hz, $NHCHCH_3$), 1.22 (3H, t, J = 7.1 Hz, OCH_2CH_3), 1.17- 1.30 (2H, m, NCH_2CH_2), 1.46-1.62 (1H, m, $CH(CH_3)_2$), 2.39-2.62 (2H, m, NCH_2CH_2), 3.45 (1H, q, J = 7.1 Hz, $NCHCH_3$), 3.52 (0.5H, s, benzyl CH_2), 3.56 (0.5H, s, benzyl CH_2), 3.74 (0.5H, s, benzyl CH_2), 3.78 (0.5H, s, benzyl CH_2), 4.02-4.19 (2H, m, OCH_2CH_3), 7.18-7.26 (1H, m, H-4), 7.27-7.35 (4H, m, H-2/3/5/6). ^{13}C NMR (100 MHz, DMSO-d_6) 14.8, 15.2, 22.7 ($CH(CH_3)_2$), 23.2 ($CH(CH_3)_2$), 25.6 ($CH(CH_3)_2$), 37.4 (NCH_2CH_2), 48.7 (NCH_2CH_2), 54.9 (benzyl-CH_2), 57.4, 60.2, 127.2 (Ar-C), 128.5 (Ar-C), 128.7 (Ar-C), 140.8 (Ar-C), 173.4 (C=O). HRMS cal. for $C_{16}H_{30}NOSi$ (ES+) m/z 278.212004 $[M+H]^+$, found 278.20918.

4.2.3 Ethyl N-benzyl-N-isopentylglycinate (10). A solution of isovaleraldehyde (**8**) (1.4 mL, 13.0 mmol) and benzylglycine ethyl ester (**9**) (0.49 mL, 2.59 mmol) in MeOH (8 mL, 0.3M) containing AcOH (0.86 mL, 10% v/v) was heated at 50°C for 1 h before $NaBH_3CN$ (0.21 g, 3.11 mmol) was added. The solution was stirred for an additional hour before being quenched with H_2O (10 mL). The material was washed with saturated $NaHCO_3$ solution (25 mL), extracted with EtOAc (3 x 15 mL), dried ($MgSO_4$), and the combined organic extracts were concentrated *in vacuo*. The crude residue was purified *via* silica gel chromatography (23:2 Hexanes:EtOAc) to give the desired compound as a colorless oil

(0.4 ... l) in [1]) 2953, 2927, 2866, 1734; ^{1}H NMR (400 MHz, DMSO-d_6) 0.80 (6H, d, J = 6.6 Hz, CH(CH_3)$_2$), 1.18 (3H, t, J = 7.1 Hz, OCH$_2$CH_3), 1.31 (2H, dt, J = 7.4, 7.0 Hz, NCH$_2$CH_2), 1.56 (1H, m, CH(CH$_3$)$_2$), 2.55 (2H, t, J = 7.4 Hz, NCH_2CH$_2$), 3.26 (2H, s, benzyl CH$_2$), 3.69 (2H, s, NCH_2CO$_2$), 4.07 (2H, q, J = 7.1 Hz, OCH_2CH$_3$), 7.19-7.27 (1H, m, H-4), 7.27-7.33 (4H, m, H-2/3/5/6).; ^{13}C NMR (100 MHz, DMSO-d_6) 14.6 (OCH$_2$CH$_3$), 23.0 (CH(CH_3)$_2$), 25.8 (CH(CH$_3$)$_2$), 36.4 (NCH$_2$CH_2), 51.6, 54.4, 58.2, 60.1, 127.4 (Ar-C), 128.6 (Ar-C), 129.1 (Ar-C), 139.7 (Ar-C), 171.2 (C=O). HRMS cal. for $C_{16}H_{26}NO_2$ (ES+) m/z 264.196354 [M+H]$^+$, found 264.192609.

4.2.4 N-(1-Ethoxy-1-oxopropan-2-yl)-3-methylbutan-1-aminium (**11**). A solution of amino acid ethyl ester **7** (0.52 g, 1.80 mmol) and Pd/C (55 mg, 0.18 mmol) in EtOH (6 mL) supplemented with concentrated HCl (180 µL) was hydrogenated according to **General Procedure A** to afford the desired compound as a white solid (1.70 g, 7.65 mmol, 99%). M.p. 98-103°C (Lit. = 105°C)[39]; IR (cm^{-1}) 2964, 2921, 2870, 2796, 2667, 2623, 2443, 1741, 1561; ^{1}H NMR (400 MHz, DMSO-d_6) 0.83 (3H, d, J = 6.7 Hz, CH(CH_3)$_2$), 0.84 (3H, d, J = 6.7 Hz, CH(CH_3)$_2$), 1.15 (3H, d, J = 6.9, NH$_2$CHCH_3), 1.19 (3H, t, J = 7.1, OCH$_2$CH_3), 1.26 (2H, dt, J = 7.2, 7.1 Hz, NH$_2$CH$_2$CH_2), 1.52-1.66 (1H, m, CH(CH$_3$)$_2$), 1.77 (2H, bs, NH$_2$), 2.31-2.43 (1H, m, NCH_2CH$_2$), 2.43-2.58 (1H, m, NCH_2CH$_2$), 3.22 (1H, q, J = 6.9 Hz, NH$_2$CHCH$_3$), 4.09 (2H, q, J = 7.1 Hz, OCH_2CH$_3$); ^{13}C NMR (100 *MHz*, DMSO-d_6) 14.6 (OCH$_2$CH$_3$), 19.1 (NH$_2$CHCH$_3$), 22.8 (CH(CH_3)$_2$), 23.2 (CH(CH_3)$_2$), 25.8 (CH(CH$_3$)$_2$), 39.2 (NH$_2$CH$_2$CH_2), 45.6 (NHCH_2CH$_2$), 56.6, 60.3, 175.7 (C=O).

4.2.5 N-(2-Ethoxy-2-oxoethyl)-3-methylbutan-1-aminium (**12**). A solution of glycine ethyl ester **10** (0.50 g, 0.19 mmol) and Pd/C (9.4 mg, 20% w/w) in EtOH (0.63 mL) containing concentrated HCl (19 µL) was hydrogenated according to **General Procedure A** to afford the desired compound as a white solid (0.32 g, 1.52 mmol, 93%). M. p. 208-210°C; IR (cm^{-1}) 2945, 2869, 2770, 2720, 2616, 2454, 1756; ^{1}H NMR (400 MHz, DMSO-d_6) 0.88 (6H, d, J = 6.4 Hz, CH(CH_3)$_2$), 1.24 (3H, t, J = 7.1 Hz, OCH$_2$CH_3), 1.47-1.71 (3H, m, CH(CH$_3$)$_2$, NCH$_2$CH_2), 2.92 (2H, t, J = 8.0 Hz, NCH_2CH$_2$), 3.95 (2H, s, NHCH_2CO$_2$), 4.21 (2H, q, J = 7.1 Hz, OCH_2CH$_3$), 9.39 (2H, s, NH$_2$); ^{13}C NMR (100 MHz, DMSO-d_6) 14.4 (OCH$_2$CH$_3$), 22.6 (CH(CH_3)$_2$), 25.8 (CH(CH$_3$)$_2$), 34.3 (NCH$_2$CH_2), 45.8, 47.1, 62.1 (OCH_2CH$_3$), 167.2 (C=O).

4.2.6 Ethyl N-(2-chloro-5-nitropyrimidin-4-yl)-N-isopentylalaninate (15). A solution of amino acid ethyl ester salt **11** (0.51 g, 2.67 mmol) in H$_2$O (4.5 mL) was added to a stirring solution of 2,4-dichloro-5-nitropyrimidine (0.44 g, 2.22 mmol) in Et$_2$O (9 mL) and reacted according to the described **General Procedure B** to afford the desired compound as a yellow oil (0.71 g, 2.06 mmol, 93%) Rf 0.79 (19:1 DCM:MeOH); IR (cm^{-1}) 2958, 2873, 1738, 1579, 1537; ^{1}H NMR (400 MHz, DMSO-d_6) 0.80-0.90 (6H, m, CH(CH_3)$_2$), 1.14 (3H, t, J = 7.1 Hz, OCH$_2$CH_3), 1.43-1.59 (6H, m, CH(CH$_3$)$_2$, NCH$_2$CH_2, NCHCH_3), 3.10- 3.25 (1H, m, NCH_2CH$_2$), 2.25-3.38 (1H, m, NCH_2CH$_2$), 4.01-4.22 (2H, m, OCH_2CH$_3$), 4.57 (1H, q, J = 6.9 Hz, NCHCH$_3$), 8.84 (1H, s, H-6); ^{13}C NMR (100 MHz, DMSO-d_6) 14.4 (OCH$_2$CH$_3$), 15.0 (NCHCH$_3$), 22.6 (CH(CH_3)$_2$), 22.7 (CH(CH_3)$_2$), 26.2 (CH(CH$_3$)$_2$), 35.1 (NCH$_2$CH_2), 50.0 (NCH_2CH$_2$), 59.2, 61.2, 131.8 (Ar-C), 153.7 (Ar-C), 157.4 (Ar-C), 159.0 (Ar-C), 170.4 (C=O). HRMS cal. for $C_{14}H_{20}ClN_4O_4$ (ES-) m/z 343.117309 [M-H]$^+$, found 343.116834.

4.2.7 Ethyl N-(2-chloro-5-nitropyrimidin-4-yl)-N-isopentylglycinate (16). A solution of amino acid ethyl ester **12** (33 mg, 0.16 mmol) in H$_2$O (0.5 mL) was added to a stirring solution of Et$_2$O (0.5 mL) and reacted according to the described **General Procedure B**. The crude material was then purified *via* silica gel chromatography (19:1 Hexanes:EtOAc) to afford the desired compound as a yellow solid (0.32 g, 0.095 mmol, 73%). Rf 0.35 (9:1 Hexanes:EtOAc); M.p. 65-68°C; IR (cm^{-1}) 2956, 2871, 1721, 1581, 1530; ^{1}H NMR (400 MHz, DMSO-d_6) 0.87 (6H, d, J = 5.7 Hz, CH(CH_3)$_2$), 1.21 (3H, t, J = 7.1 Hz, OCH$_2$CH_3), 1.43-1.59 (3H, m, CH(CH$_3$)$_2$, NCH$_2$CH_2), 3.18-3.59 (2H, m, NCH_2CH$_2$), 4.16 (2H, q, J = 7.1, OCH_2CH$_3$), 4.31 (2H, s, NCH_2CO$_2$), 8.84 (1H, s, H-6); ^{13}C NMR (100 MHz, DMSO-d_6) 14.5 (OCH$_2$CH$_3$), 22.7 (CH(CH_3)$_2$), 26.1 (CH(CH$_3$)$_2$), 34.6 (NCH$_2$CH_2), 51.1, 51.9, 61.3 (OCH_2CH$_3$), 131.6 (Ar-C), 154.5 (Ar-C), 157.3 (Ar-C), 159.6 (Ar-C), 168.5 (C=O). HRMS cal. for $C_{13}H_{20}ClN_4O_4$ (ES+) m/z 331.117309 [M+H]$^+$, found 331.121466.

4.2.8 Ethyl (2-chloro-5-nitropyrimidin-4-yl)alaninate (17). A solution of alanine ethyl ester **13** (50.8 mg, 0.33 mmol) in H$_2$O (0.6 mL) was added to a stirring solution of 2,4-dichloro-5-nitropyrimidine (53 mg, 0.27 mmol) in Et$_2$O (1.1 mL) and reacted according to the described **General Procedure B**. The crude material was then purified *via* silica gel chromatography (19:1 Hexanes:EtOAc) to afford desired compound as a white solid (0.52 g, 0.19 mmol, 70%). Rf 0.3 (19:1 DCM:MeOH); M. p. 58-60°C; IR (cm^{-1}) 3337, 2989, 1731, 1610, 1573, 1517; ^{1}H NMR (400 MHz, DMSO-d_6) 1.20 (3H, t, J = 7.1 Hz, OCH$_2$CH_3), 1.51 (3H, d, J = 7.1 Hz, NHCHCH_3), 4.17 (2H, q, J = 7.1, OCH_2CH$_3$), 4.72-4.83 (1H, dq, J =7.1, 7.1 Hz, NHCHCH$_3$), 9.07 (1H, s, NH), 9.09 (1H, s, H-6); ^{13}C NMR (100 MHz, DMSO-d_6) 14.5 (OCH$_2$CH$_3$), 17.0 (NHCHCH$_3$), 50.5 (NHCHCH$_3$), 61.6 (127.9 (Ar-C), 154.8 (Ar-C), 157.9 (Ar-C), 162.5 (Ar-C), 171.5 (C=O). HRMS cal. for $C_9H_{12}ClN_4O_4$ (ES+) m/z 275.054709 [M+H]$^+$, found 275.057639.

4.2.9 2-Chloro-8-isopentyl-7-methyl-7,8-dihydropteridin-6(5H)-one (18). A solution of amino acid ethyl ester **15** (0.12 g, 0.29 mmol) in acetic acid (1.5 mL) was heated to 70°C prior to the addition of iron powder (99 mg, 1.45 mmol,). The solution was reacted according to **General Procedure C** to afford the desired compound as a yellow solid (61 mg, 0.23 mmol, 79%). Rf 0.32 (19:1 DCM:MeOH); M. p. 182-184°C (Lit. = 182-185°C)[39]; IR (cm^{-1}) 3743, 3172, 3109, 3050, 2956, 2925, 2872, 1675, 1606; ^{1}H NMR (400 MHz, DMSO-d_6) 0.91 (3H, d, J = 6.3 Hz, CH(CH_3)$_2$), 0.92 (3H, d, J = 6.3 Hz, CH(CH_3)$_2$), 1.36 (3H, d, J = 6.8 Hz, NCHCH_3), 1.39-1.64 (3H, m, NCH$_2$CH_2, CH(CH$_3$)$_2$), 3.13-3.22 (1H, m, NCH_2CH$_2$), 3.81-3.93 (1H, m, NCH_2CH$_2$), 4.24 (1H, q, J = 6.8 Hz, NCHCH$_3$), 7.55 (1H, s, H-4), 10.75 (1H, s, NH); ^{13}C NMR (100 MHz, DMSO-d_6) 18.1 (NCHCH$_3$), 22.7 (CH(CH_3)$_2$), 22.9 (CH(CH_3)$_2$), 25.9 (CH(CH$_3$)$_2$), 35.6 (NCH$_2$CH_2), 43.2 (NCH_2CH$_2$), 56.4 (NCHCH$_3$), 119.2 (Ar-C), 138.2 (Ar-C), 151.2 (Ar-C), 152.8 (Ar-C), 165.6 (C=O). HRMS cal. for $C_{12}H_{18}ClN_4O$ (ES+) m/z 269.116914 [M+H]$^+$, found 269.111913.

4.2.10 2-Chloro-8-isopentyl-7,8-dihydropteridin-6(5H)-one (**19**). A solution of pteridinone **16** (0.24 g, 0.73 mmol) in acetic acid (4 mL) was heated to 70°C before iron powder (0.22 g, 3.63 mmol) was added. The solution was then reacted according to **General Procedure C** to afford the desired compound as a white solid (0.14 g, 0.56 mmol, 76%). Rf 0.39 (19:1 DCM:MeOH); M. p. 185-187°C; IR (cm^{-1}) 3110, 3061, 2953, 2922, 2865, 1693, 1598, 1565, 1532; ^{1}H NMR (400 MHz, DMSO-d_6) 0.92 (6H, d, J = 6.3 Hz, CH(CH_3)$_2$), 1.37-1.65 (3H, m, CH(CH$_3$)$_2$, NCH$_2$CH_2), 3.49 (2H, t, J = 7.3 Hz, NCH_2CH$_2$), 4.13 (2H, s, NCH_2CO$_2$), 7.50 (1H, s, H-4), 10.74 (1H, s, NH); ^{13}C NMR (100 MHz, DMSO-d_6) 22.8 (CH(CH_3)$_2$), 25.7 (CH(CH$_3$)$_2$), 34.2 (NCH$_2$CH_2), 44.9 (NCH_2CH$_2$), 50.1 (NCH_2CO), 119.5 (Ar-C), 137.7 (Ar-C), 151.5

(Ar- Hz, (ES+) m/z 255.101264 $[M+H]^+$, found 255.096829.

4.2.11 2-Chloro-7-methyl-7,8-dihydropteridin-6(5H)-one (20). A solution of pteridinone **17** (0.60 g, 2.19 mmol) in acetic acid (11 mL) was heated to 70°C prior to the addition of iron powder (0.64 g, 11.0 mmol). The solution was then reacted according to **General Procedure C** to afford the desired compound as a white solid (0.32 g, 1.16 mmol, 73%). Rf 0.25 (19:1 DCM:MeOH); M. p. 250-265°C decomposed; IR (cm^{-1}) 3206, 3099, 2921, 1678, 1609, 1554; ^{1}H NMR (400 MHz, DMSO-d_6) 1.32-1.43 (3H, m, NHCHCH_3), 4.18-4.32 (1H, m, NHCHCH$_3$), 7.53 (1H, s, H-4), 7.54 (1H, s, NH), 8.45 (1H, s, NHCHCH$_3$), 10.6 (1H, s, NHCO). ^{13}C NMR (100 MHz, DMSO-d_6) 20.0 (NHCHCH$_3$), 51.0 (NHCHCH$_3$), 118.8 (Ar-C), 138.1 (Ar-C), 152.6 (Ar-C), 152.7 (Ar-C), 166.3 (C=O). HRMS cal. for $C_7H_8ClN_4O$ (ES+) m/z 199.038664 $[M+H]^+$, found 199.040771.

4.2.12 2-Chloro-8-isopentyl-5,7-dimethyl-7,8-dihydropteridin-6(5H)-one (21). To an oven dried flask cooled under N_2 was added a solution of pteridinone **18** (51 mg, 0.19 mmol) in DMA (0.5 mL). The solution was cooled to -15°C and NaH (10 mg, 0.21 mmol) followed by MeI (46 µL, 0.74 mmol) were added. The solution was reacted according to **General Procedure D** to afford the desired compound as a yellow oil (52 mg, 0.18 mmol, 99%). Rf 0.63 (9:1 DCM:MeOH); IR (cm^{-1}) 3057, 2955, 2928, 2869, 1679, 1579, 1519; ^{1}H NMR (400 MHz, DMSO-d_6) 0.91 (3H, d, J = 6.2 Hz, CH(CH_3)$_2$), 0.92 (3H, d, J = 6.2 Hz, CH(CH_3)$_2$), 1.34 (3H, d, J = 6.8 Hz, NCHCH_3), 1.40-1.63 (3H, m, NCH$_2$CH_2, CH(CH$_3$)$_2$), 3.11-3.20 (1H, m, NCH_2CH$_2$), 3.22 (3H, s, NCH_3), 3.82-3.97 (1H, m, NCH_2CH$_2$), 4.36 (1H, q, J = 6.8 Hz, NCHCH$_3$), 7.86 (1H, s, H-4). ^{13}C NMR (100 MHz, DMSO-d_6) 18.2 (NCHCH$_3$), 22.7 (CH(CH$_3$)$_2$), 22.9 (CH(CH$_3$)$_2$), 25.9 (CH(CH$_3$)$_2$), 28.5 (N-methyl), 35.6 (NCH$_2C$H$_2$), 43.3 (NCH$_2$CH$_2$), 56.4 (NCHCH$_3$), 121.1 (Ar-C), 138.8 (Ar-C), 151.6 (Ar-C), 153.2 (Ar-C), 164.6 (C=O).

4.2.13 2-Chloro-8-isopentyl-5-methyl-7,8-dihydropteridin-6(5H)-one (**22**). To an oven dried flask cooled under N_2 was added a solution of cyclized pteridinone **19** (31 mg, 0.12 mmol) in DMA (0.5 mL). The solution was cooled to -15°C and NaH (51 mg, 0.13 mmol) was added. The reaction mixture was stirred for 10 min and MeI (9 uL, 0.14 mmol) was added. The solution was reacted according to **General Procedure D** and the crude residue was purified *via* silica gel chromatography (97:3 DCM:MeOH) to afford the desired compound as a white solid (0.25 g, 0.092 mmol, 76%). Rf 0.57 (19:1 DCM:MeOH); M. p. 132-135°C; IR (cm^{-1}) 3061, 2943, 2871, 1675, 1565, 1529; ^{1}H NMR (400 MHz, DMSO-d_6) 0.92 (6H, d, J = 6.5 Hz, CH(CH_3)$_2$), 1.46 (2H, dt, J = 7.5, 6.8 Hz, NCH$_2$CH_2), 1.45-1.65 (1H, m, CH(CH$_3$)$_2$), 3.20 (3H, s, NCH_3), 3.51 (2H, t, J = 7.5 Hz, NCH_2CH$_2$), 4.23 (2H, s, NCH_2CO$_2$), 7.78 (1H, s, H-4). ^{13}C NMR (100 MHz, DMSO-d_6) 22.8 (CH(CH$_3$)$_2$), 25.7 (CH(CH$_3$)$_2$), 28.0 (NCH$_3$), 34.1 (NCH$_2C$H$_2$), 44.9 (NCH$_2$CH$_2$), 50.1 (NCH$_2$CO), 121.3 (Ar-C), 138.1 (Ar-C), 151.9 (Ar-C), 153.1 (Ar-C), 161.8 (C=O). HRMS cal. $C_{12}H_{18}ClN_4O$ (ES+) m/z 269.116914 $[M+H]^+$, found 269.116008.

4.2.14 2-Chloro-5,7-dimethyl-7,8-dihydropteridin-6(5H)-one (23). To an oven dried flask cooled under N_2 was added a solution of pteridinone precursor **20** (0.15 g, 0.76 mmol) in DMA (2 mL). The solution was cooled to -15°C and NaH (31 mg, 0.76 mmol) was added. The reaction mixture was stirred for 10 min and MeI (56.4 µL, 1.51 mmol) added. The solution was reacted according to **General Procedure D** and the crude residue was purified *via* silica gel chromatography (9:1 DCM:MeOH) to afford the desired compound as a. off white-solid (0.076 g, 0.36 mmol, 46%). Rf 0.57 (19:1 DCM:MeOH); M. p. 257-267°C decomposed; IR (cm^{-1}) DMSO-d_6) 1.37 (3H, d, J = 6.8 Hz, NHCHCH_3), 3.20 (3H, s, NCH_3), 4.32 (1H, q, J = 6.8 Hz, NHCHCH$_3$), 7.81 (1H, s, H-4), 8.59 (1H, s, NH). ^{13}C NMR (100 MHz, DMSO-d_6) 20.3 (NHCHCH$_3$), 28.4 (NCH$_3$), 51.0 (NHCHCH$_3$), 120.7 (Ar-C), 138.7 (Ar-C), 153.0 (Ar-C), 153.1 (Ar-C), 165.3 (C=O). HRMS cal. $C_8H_{10}ClN_4O$ (ES+) m/z 213.054314 $[M+H]^+$, found 213.056105.

4.2.15 2-((3,5-Difluorophenyl)amino)-8-isopentyl-5,7-dimethyl-7,8-dihydropteridin-6(5H)-one (24). Pteridinone heterocycle **21** (53 mg, 0.18 mmol), 3,5-Difluoroaniline (47.5 mg, 0.354 mmol) and TFA (68 µL, 0.885 mmol) were taken up in TFE (2 mL) and reacted according to the described **General Procedure E**. Purification *via* silica gel chromatography (1:1 Hexanes:EtOAc) afforded the target compound as a white solid (30 mg, 0.08 mmol, 43%). Rf 0.22 (1:1 Hex: EtOAc); M. p. 137-139°C ; IR (cm^{-1}) 3275, 2957, 2871, 1670, 1629, 1602, 1575, 1531; ^{1}H NMR (400 MHz, DMSO-d_6) 0.92 (3H, d, J = 6.7 Hz, CH(CH_3)$_2$), 0.93 (3H, d, J = 6.7 Hz, CH(CH_3)$_2$), 1.30 (3H, d, J = 6.8 Hz, NCHCH_3), 1.43-1.70 (3H, m, CH(CH$_3$)$_2$, NCH$_2$CH_2), 3.11-3.23 (1H, m, NCH_2CH$_2$), 3.24 (3H, s, NCH$_3$), 3.93-4.06 (1H, m, NCH_2CH$_2$), 4.28 (1H, q, J = 6.8 Hz, NCHCH$_3$), 6.62 (1H, m, H-4'), 7.49 (2H, d, J = 8.7 Hz, H-2'/6'), 7.85 (1H, s, H-4), 9.54 (1H, s, NH); ^{13}C NMR (100 MHz, DMSO-d_6) 17.6 (NCHCH$_3$), 22.9 (CH(CH$_3$)$_2$), 22.9 (CH(CH$_3$)$_2$), 26.2 (CH(CH$_3$)$_2$), 28.2 (NCH$_3$), 36.0 (NCH$_2C$H$_2$), 43.5 (NCH$_2$CH$_2$), 56.6 (NCHCH$_3$), 95.4 (dd, J_{CF} = 26.6 Hz, Ar-C), 100.7 (d, J_{CF} = 29.6 Hz, Ar-C), 115.7 (Ar-C), 138.9 (Ar-C), 144.4 (dd, J_{CF} = 14.4, 14.2 Hz, Ar-C), 151.0 (Ar-C, 155.4 (Ar-C), 163 (dd, J_{CF} = 240.8, 16.1 Hz, Ar-C), 164.3 (C=O). HRMS cal. $C_{19}H_{24}F_2N_5O$ (ES+) m/z 376.194891 $[M+H]^+$, found 376.190797.

4.2.16 2-((3,5-Difluoro-4-methoxyphenyl)amino)-8-isopentyl-5,7-dimethyl-7,8-dihydropteridin-6(5H)-one (24). Pteridinone heterocycle **21** (51 mg, 0.177 mmol), 3,5-Difluoro-4-methoxyaniline (57 mg, 0.354 mmol) and TFA (68 µL, 0.885 mmol) were taken up in TFE (2 mL) and reacted according to the described **General Procedure E**. Purification by amine chromatography (1:1 Hexanes:EtOAc) afforded the target compound as a white solid (39.9 mg, 0.098 mmol, 27%). Rf 0.22 (1:1 Hexanes:EtOAc); M. p. 138-141°C; IR (cm^{-1}) 3272, 3194, 3116, 2956, 2931, 2870, 1667, 1610, 1574, 1510; ^{1}H NMR (400 MHz, DMSO-d_6) 0.91 (3H, d, J = 6.9 Hz, CH(CH_3)$_2$), 0.93 (3H, d, J = 6.9 Hz, CH(CH_3)$_2$), 1.28 (3H, d, J = 6.8 Hz, NCHCH_3), 1.43-1.69 (3H, m, CH(CH$_3$)$_2$, NCH$_2$CH_2), 3.09-3.22 (1H, m, NCH_2CH$_2$), 3.22 (3H, s, NCH$_3$), 3.82 (3H, s, OCH_3), 3.93-4.04 (1H, m, NCH_2CH$_2$), 4.27 (1H, q, J = 6.8 Hz, NCHCH$_3$), 7.52 (2H, d, J = 11.4 Hz, H-2'/6'), 7.83 (1H, s, H-4), 9.35 (1H, s, NH); ^{13}C NMR (100 MHz, DMSO-d_6) 17.5 (NCHCH$_3$), 22.9 (CH(CH$_3$)$_2$), 22.9 (CH(CH$_3$)$_2$), 26.2 (CH(CH$_3$)$_2$), 28.2 (NCH$_3$), 36.0 (NCH$_2C$H$_2$), 43.4 (NCH$_2$CH$_2$), 56.6 (NCHCH$_3$), 62.5 (OCH$_3$), 101.9 (d, J_{CF} = 27.5 Hz, Ar-C), 115.5 (Ar-C), 129.2 (dd, J_{CF} = 15.3 Hz, Ar-C), 137.8 (dd, J_{CF} = 13.4 Hz, Ar-C), 138.9 (Ar-C), 151.0 (Ar-C), 155.5 (Ar-C), 156.8 (dd, , J_{CF} = 241.9, 8.3, Ar-C), 164.3 (C=O). HRMS cal. $C_{20}H_{26}F_2N_5O_2$ (ES+) m/z 406.205456 $[M+H]^+$, found 406.199354.

4.2.17 2-((4-(Hydroxymethyl)phenyl)amino)-8-isopentyl-5,7-dimethyl-7,8-dihydropteridin-6(5H)-one (26). To a solution of TIPS-protected pteridinone intermediate **44** (96 mg, 0.182 mmol) in THF (1.8 mL, 0.1M) stirring at -15°C was added a 1M solution of TBAF (0.22 ml, 0.219 mmol) dropwise. The reaction was reacted for 2 h before the solvent was removed *in vacuo*. The crude material was purified *via* silica gel chromatography (19:1 DCM:MeOH) to afford the desired compound as a white solid (41

mg, 178°C; IR (cm^{-1}) 3337, 3256, 3187, 2930, 2850, 1638, 1610, 1572, 1532; ^{1}H NMR (400 MHz, DMSO-d_6) 0.93 (3H, d, J = 6.4 Hz, CH(CH_3)$_2$), 0.96 (3H, d, J = 6.4 Hz, CH(CH_3)$_2$), 1.27 (3H, d, J = 6.8 Hz, NCHCH_3), 1.45-1.69 (3H, m, CH(CH$_3$)$_2$, NCH$_2$CH_2), 3.07-3.18 (1H, m, NCH_2CH$_2$), 3.22 (3H, s, NCH$_3$), 3.96-4.09 (1H, m, NCH_2CH$_2$), 4.25 (1H, q, J = 6.8 Hz, NCHCH$_3$), 4.40 (2H, d, J = 5.6 Hz, CH_2OH), 4.99 (1H, t, J = 5.6 Hz, CH$_2$OH), 7.15 (2H, d, J = 8.5 Hz, H-3'/5'), 7.68 (2H, d, J = 8.5 Hz, H-2'/6'), 7.79 (1H, s, H-4), 9.03 (1H, s, NH); ^{13}C NMR (100 MHz, DMSO-d_6) 17.4 (NCHCH$_3$), 23.0 (CH(CH$_3$)$_2$), 23.0 (CH(CH$_3$)$_2$), 26.3 (CH(CH$_3$)$_2$), 28.2 (NCH$_3$), 36.1 (NCH$_2C$H$_2$), 43.3 (NCH$_2$CH$_2$), 56.6 (NCHCH$_3$), 63.3 (CH$_2$OH), 114.7 (Ar-C), 118.1 (Ar-C), 127.3 (Ar-C), 134.9 (Ar-C), 139.2 (Ar-C), 140.5 (Ar-C), 151.0 (Ar-C), 156.2 (Ar-C), 164.3 (C=O). HRMS cal. $C_{20}H_{28}N_5O_2$ (ES+) m/z 370.224299 [M+H]$^+$, found 370.218594.

4.2.18 2-((4-Hydroxyphenyl)amino)-8-isopentyl-5,7-dimethyl-7,8-dihydropteridin-6(5H)-one (**27**). To a solution of TIPS-protected pteridinone intermediate **50** (87 mg, 0.17 mmol) in THF (1.7 mL, 0.1M) stirring at -15°C was added a 1M solution of TBAF in THF (0.2 mL, 0.204 mmol) dropwise. The solution was reacted for 2 h before the solvent was concentrated *in vacuo*. The crude material was purified *via* silica gel chromatography (19:1 DCM:MeOH) to afford the desired compound as a brown solid (36.9 mg, 0.104 mmol, 61%). Rf 0.23 (97:3 DCM:MeOH); M. p. 260-261°C; IR (cm^{-1}) 3278, 2955, 2865, 1646, 1606, 1539, 1505; ^{1}H NMR (400 MHz, DMSO-d_6) 0.91 (3H, d, J = 6.4 Hz, CH(CH_3)$_2$), 0.94 (3H, d, J = 6.4 Hz, CH(CH_3)$_2$), 1.25 (3H, d, J = 6.8 Hz, NCHCH_3), 1.40-1.67 (3H, m, CH(CH$_3$)$_2$, NCH$_2$CH_2), 3.01-3.13 (1H, m, NCH_2CH$_2$), 3.21 (3H, s, NCH$_3$), 3.92-4.05 (1H, m, NCH_2CH$_2$), 4.22 (1H, q, J = 6.8 Hz, NCHCH$_3$), 6.63 (2H, d, J = 8.9 Hz, H-3'/5'), 7.46 (2H, d, J = 8.9 Hz, H-2'/6'), 7.74 (1H, s, H-4), 8.72 (1H, s, NH), 8.89 (1H, s, OH); ^{13}C NMR (100 MHz, DMSO-d_6) 17.3 (NCHCH$_3$), 22.9 (CH(CH$_3$)$_2$), 23.0 (CH(CH$_3$)$_2$), 26.3 (CH(CH$_3$)$_2$), 28.2 (NCH$_3$), 36.1 (NCH$_2C$H$_2$), 43.2 (NCH$_2$CH$_2$), 56.6 (NCHCH$_3$), 114.2 (Ar-C), 115.2 (Ar-C), 120.6 (Ar-C), 133.5 (Ar-C), 139.4 (Ar-C), 140.5 (Ar-C), 151.0 (Ar-C), 156.5 (Ar-C), 164.32(C=O). HRMS cal. $C_{19}H_{26}N_5O_2$ (ES+) m/z 356.20865 [M+H]$^+$, found 356.202489.

4.2.19 2-((3-Fluoro-4-hydroxyphenyl)amino)-8-isopentyl-5,7-dimethyl-7,8-dihydropteridin-6(5H)-one (28). Monofluoro-methoxy pteridinone **51** (82 mg, 0.206 mmol) in DCM (1 mL) was reacted with 1M BBr_3 according to **General Procedure F**. The crude residue was purified *via* silica gel chromatography (19:1 DCM:MeOH) to give the desired compound as a white solid (24.5 mg, 0.048 mmol, 32%). Rf 0.4 (19:1 DCM:MeOH); M. p. 225-227°C; IR (cm^{-1}) 3271, 2956, 2928, 1646, 1606, 1584, 1539; ^{1}H NMR (400 MHz, DMSO-d_6) 0.90 (3H, d, J = 6.7 Hz, CH(CH_3)$_2$), 0.92 (3H, d, J = 6.7 Hz, CH(CH_3)$_2$), 1.25 (3H, d, J = 6.7 Hz, NCHCH_3), 1.42-1.70 (3H, m, CH(CH$_3$)$_2$, NCH$_2$CH_2), 3.06-3.17 (1H, m, NCH_2CH$_2$), 3.21 (3H, s, NCH$_3$), 3.91-4.04 (1H, m, NCH_2CH$_2$), 4.26 (1H, q, J = 6.7 Hz, NCHCH$_3$), 6.81 (1H, dd, J = 9.3, 9.3 Hz, H-5'), 7.13-7.26 (1H, m, H-6'), 7.63 (1H, dd, J = 14.1, 2.0 Hz, H-2'), 7.75 (1H, s, H-4), 9.04 (1H, s, NH), 9.26 (1H, s, OH); ^{13}C NMR (100 MHz, DMSO-d_6) 17.4 (NCHCH$_3$), 22.9 (CH(CH$_3$)$_2$), 26.2 (CH(CH$_3$)$_2$), 28.2 (NCH$_3$), 36.1 (NCH$_2C$H$_2$), 43.3 (NCH$_2$CH$_2$), 56.6 (NCHCH$_3$), 107.2 (d, J_{CF} = 23.3 Hz, Ar-C), 114.8 (d, J_{CF} = 2.8 Hz, Ar-C), 114.9 (Ar-C), 117.8 (d, J_{CF} = 4.0 Hz, Ar-C), 134.1 (d, J_{CF} = 9.4 Hz, Ar-C), 138.8 (d, J_{CF} = 12.7 Hz, Ar-C), 138.9 (Ar-C), 150.9 (d, J_{CF} = 237.2 Hz, Ar-C), 151.0 (Ar-C), 156.0 (Ar-C), 164.2 (C=O). HRMS cal. $C_{19}H_{25}FN_5O_2$ (ES+) m/z 374.199228 [M+H]$^+$, found 374.192346.

4.2.20 2-((3-Chloro-4-hydroxyphenyl)amino)-8-isopentyl-5,7-dimethyl-7,8-dihydropteridin-6(5H)-one (29). Monochloro-methoxy pteridinone **52** (80.7 mg, 0.198 mmol) in DCM (1 mL) was reacted with 1M BBr_3 according to **General Procedure F**. The crude residue was purified *via* silica gel chromatography (19:1 DCM:MeOH) to give the desired compound as a gray solid (19.8 mg, 0.051 mmol, 26%). Rf 0.33 (19:1 DCM:MeOH); M. p. 220-230°C decomposed; IR (cm^{-1}) 3183, 3126, 2952, 2865, 1638, 1611, 1577, 1513; ^{1}H NMR (400 MHz, DMSO-d_6) 0.91 (3H, d, J = 6.7 Hz, CH(CH_3)$_2$), 0.93 (3H, d, J = 6.7 Hz, CH(CH_3)$_2$), 1.26 (3H, d, J = 6.7 Hz, NCHCH_3), 1.43-1.69 (3H, m, CH(CH$_3$)$_2$, NCH$_2$CH_2), 3.05-3.16 (1H, m, NCH_2CH$_2$), 3.21 (3H, s, NCH$_3$), 3.96-4.07 (1H, m, NCH_2CH$_2$), 4.22 (1H, q, J = 6.7 Hz, NCHCH$_3$), 6.83 (1H, d, J = 8.8 Hz, H-5'), 7.39 (1H, dd, J = 8.8, 2.6 Hz, H-6'), 7.78 (1H, s, H-4), 7.81 (1H, d, J = 2.6 Hz, H-2'), 8.92 (1H, s, NH), 9.54 (1H, s, OH); ^{13}C NMR (100 MHz, DMSO-d_6) 17.3 (NCHCH$_3$), 22.9 (CH(CH$_3$)$_2$), 23.0 (CH(CH$_3$)$_2$), 26.1 (CH(CH$_3$)$_2$), 28.2 (NCH$_3$), 36.1 (NCH$_2C$H$_2$), 43.0 (NCH$_2$CH$_2$), 56.5 (NCHCH$_3$), 114.7 (Ar-C), 116.8 (Ar-C), 118.8 (Ar-C), 119.5 (Ar-C), 120.0 (Ar-C), 134.5 (Ar-C), 139.2 (Ar-C), 147.4 (Ar-C), 151.1 (Ar-C), 156.1 (Ar-C), 164.2 (C=O). HRMS cal. $C_{19}H_{25}ClN_5O_2$ (ES+) m/z 390.169678 [M+H]$^+$, found 390.161688.

4.2.21 2-((3-Bromo-4-hydroxyphenyl)amino)-8-isopentyl-5,7-dimethyl-7,8-dihydropteridin-6(5H)-one (**30**). Monobromo-methoxy pteridinone **53** (84.8 mg, 0.178 mmol) in DCM (1 mL) was reacted with 1M BBr_3 according to **General Procedure F**. The crude residue was purified *via* silica gel chromatography (47:3 DCM:MeOH) to give the desired compound as a gray solid (28.5 mg, 0.066 mmol, 35%). Rf 0.42 (47:3 DCM:MeOH); M. p. 220-235°C decomposed; IR (cm^{-1}) 3168, 3122, 2948, 1639, 1607, 1574, 1509; ^{1}H NMR (400 MHz, DMSO-d_6) 0.91 (3H, d, J = 6.6 Hz, CH(CH_3)$_2$), 0.93 (3H, d, J = 6.6 Hz, CH(CH_3)$_2$), 1.26 (3H, d, J = 6.7 Hz, NCHCH_3), 1.42-1.70 (3H, m, CH(CH$_3$)$_2$, NCH$_2$CH_2), 3.02-3.15 (1H, m, NCH_2CH$_2$), 3.21 (3H, s, NCH$_3$), 3.96-4.08 (1H, m, NCH_2CH$_2$), 4.22 (1H, q, J = 6.7 Hz, NCHCH$_3$), 6.82 (1H, d, J = 8.8 Hz, H-5'), 7.44 (1H, dd, J = 8.8, 2.5 Hz, H-6'), 7.77 (1H, s, H-4), 7.95 (1H, d, J = 2.5 Hz, H-2'), 8.91 (1H, s, NH), 9.62 (1H, s, OH); ^{13}C NMR (100 MHz, DMSO-d_6) 17.3 (NCHCH$_3$), 22.9 (CH(CH$_3$)$_2$), 23.1 (CH(CH$_3$)$_2$), 26.1 (CH(CH$_3$)$_2$), 28.2 (NCH$_3$), 36.1 (NCH$_2C$H$_2$), 43.0 (NCH$_2$CH$_2$), 56.5 (NCHCH$_3$), 109.1 (Ar-C), 114.7 (Ar-C), 116.4 (Ar-C), 119.5 (Ar-C), 123.0 (Ar-C), 134.7 (Ar-C), 139.1 (Ar-C), 148.5 (Ar-C), 151.1 (Ar-C), 156.1 (Ar-C), 164.2 (C=O). HRMS cal. $C_{19}H_{25}BrN_5O_2$ (ES+) m/z 434.119161 [M+H]$^+$, found 434.112483.

4.2.22 2-((3,5-Dichloro-4-hydroxyphenyl)amino)-8-isopentyl-5,7-dimethyl-7,8-dihydropteridin-6(5H)-one (31). Pteridinone heterocycle **21** (104 mg, 0.368 mmol), 4-Amino-2,6-dichlorophenol (**X**) (131 mg, 0.735 mmol) and TFA (141 µL, 1.84 mmol) were taken up in TFE (3.8 mL) and reacted according to the described **General Procedure E**. Purification *via* silica gel chromatography (17:3 DCM:MeOH) and subsequent trituration with MeOH afforded the desired compound as a brown solid (61 mg, 0.143 mmol, 39%). Rf 0.46 (1:2 Hexanes:EtOAc); M. p. 185-187°C decomposed; IR (cm^{-1}) 3373, 2847, 2865, 1683, 1612, 1593, 1563, 1526; ^{1}H NMR (400 MHz, DMSO-d_6) 0.90 (3H, d, J = 6.9 Hz, CH(CH_3)$_2$), 0.92 (3H, d, J = 6.9 Hz, CH(CH_3)$_2$), 1.27 (3H, d, J = 6.7 Hz, NCHCH_3), 1.43-1.70 (3H, m, CH(CH$_3$)$_2$, NCH$_2$CH_2), 3.06-3.19 (1H, m, NCH_2CH$_2$), 3.22 (3H, s, NCH$_3$), 3.97-4.11 (1H, m, NCH_2CH$_2$), 4.24 (1H, q, J = 6.7 Hz, NCHCH$_3$), 7.78 (2H, s, H-2'/6'), 7.82 (1H, s, H-4), 9.12 (1H, s NH), 9.45 (1H, s, OH); ^{13}C NMR (100 MHz, DMSO-d_6) 17.3 (NCHCH$_3$), 22.8 (CH(CH$_3$)$_2$), 23.1 (CH(CH$_3$)$_2$), 26.0 (CH(CH$_3$)$_2$), 28.2 (NCH$_3$), 36.0 (NCH$_2C$H$_2$), 43.0 (NCH$_2$CH$_2$), 56.4 (NCHCH$_3$), 115.2 (Ar-C), 118.3 (Ar-C), 122.8 (Ar-C), 135.3 (Ar-C), 139.0 (Ar-C), 142.9

(Ar-C), 127.1 (dd, J_{CF} = 16.7, 16.5 Hz, Ar-C), 133.7 (dd, J_{CF} = 12.9, 12.9 Hz, Ar-C), 138.4 (Ar-C), 151.1 (Ar-C), 152.7 (dd, J_{CF} = 237.6, 9.1 Hz, Ar-C), 155.6 (Ar-C), 164.3 (C=O). HRMS cal. $C_{19}H_{24}Cl_2N_5O_2$ (ES+) m/z 424.130706 $[M+H]^+$, found 424.122146.

4.2.23 2-((3,5-Dibromo-4-hydroxyphenyl)amino)-8-isopentyl-5,7-dimethyl-7,8-dihydropteridin-6(5H)-one (**32**). Pteridinone heterocycle **21** (81 mg, 0.287 mmol), aniline **42** (157 mg, 0.574 mmol) and TFA (110 µL, 1.43 mmol) were taken up in TFE (3 mL) and reacted according to the described **General Procedure E**. Purification *via* silica gel chromatography (9:1 DCM:MeOH) and subsequent trituration with MeOH afforded the target compound as a brown solid (81 mg, 0.16 mmol, 61%). Rf 0.42 (1:2 Hexanes:EtOAc); M. p. 184-186°C; IR (cm^{-1}) 3375, 2957, 2865, 1683, 1612, 1591, 1560, 1521; ^{1}H NMR (400 MHz, DMSO-d_6) 0.90 (3H, d, J = 6.9 Hz, CH(CH_3)$_2$), 0.92 (3H, d, J = 6.9 Hz, CH(CH_3)$_2$), 1.27 (3H, d, J = 6.7 Hz, NHCHCH_3), 1.41-1.73 (3H, m, CH(CH$_3$)$_2$, NCH$_2$CH_2), 3.02-3.18 (1H, m, NCH_2CH$_2$), 3.22 (3H, s, NCH_3), 3.97-4.13 (1H, m, NCH_2CH$_2$), 4.23 (1H, q, J = 6.7 Hz, NCHCH$_3$), 7.82 (1H, s, H-4), 7.98 (2H, s, H-2'/6'), 9.10 (1H, s, NH) 1.30 (1H, bs, OH); ^{13}C NMR (100 MHz, DMSO-d_6) 17.2 (NCHCH$_3$), 22.9 (CH(CH$_3$)$_2$), 23.2 (CH(CH$_3$)$_2$), 26.0 (CH(CH$_3$)$_2$), 28.2 (NCH$_3$), 36.0 (NCH$_2C$H$_2$), 42.8 (NCH$_2$CH$_2$), 56.4 (NCHCH$_3$), 112.6 (Ar-C), 115.2 (Ar-C), 121.9 (Ar-C), 136.4 (Ar-C), 139.1 (Ar-C), 144.6 (Ar-C), 151.1 (Ar-C), 155.6 (Ar-C), 164.3 (C=O). HRMS cal. $C_{19}H_{24}Br_2N_5O_2$ (ES+) m/z 512.029671 $[M+H]^+$, found 512.025409.

4.2.24 2-((3,5-Difluoro-4-hydroxyphenyl)amino)-8-isopentyl-7-methyl-7,8-dihydropteridin-6(5H)-one (33). Pteridinone heterocycle **18** (83 mg, 0.298 mmol), aniline **41** (88 mg, 0.752 mmol) and TFA (114 µL, 1.49 mmol) were taken up in TFE (3 mL) and reacted according to the described **General Procedure E**. Purification *via* silica gel chromatography (97:3 DCM:MeOH) afforded the target compound as a brown solid (77.5 mg, 0.205 mmol, 67%). Rf 0.26 (1:2 Hexanes:EtOAc); M. p. 170-210°C decomposed; IR (cm^{-1}) 2951, 1677, 1621, 1581, 1513; ^{1}H NMR (400 MHz, DMSO-d_6) 0.91 (3H, d, J = 6.8 Hz, CH(CH_3)$_2$), 0.93 (3H, d, J = 6.8 Hz, CH(CH_3)$_2$), 1.30 (3H, d, J = 6.7 Hz, NHCHCH_3), 1.41-1.72 (3H, m, CH(CH$_3$)$_2$, NCH$_2$CH_2), 3.07-3.20 (1H, m, NCH_2CH$_2$), 3.89-4.01 (1H, m, NCH_2CH$_2$), 4.13 (1H, q, J = 6.7 Hz, NCHCH$_3$), 7.35-7.47 (2H, d, J = 10.6 Hz, H-2'/6'), 7.53 (1H, s, H-4), 9.05 (1H, s, NH), 9.39 (1H, s, OH), 10.39 (1H, s, NHCO); ^{13}C NMR (100 MHz, DMSO-d_6) 17.5 (NCHCH$_3$), 22.9 (CH(CH$_3$)$_2$), 26.2 (CH(CH$_3$)$_2$), 36.0 (NCH$_2C$H$_2$), 43.3 (NCH$_2$CH$_2$), 56.6 (NCHCH$_3$), 101.8 (d, J_{CF} = 27.2 Hz, Ar-C), 112.8 (Ar-C), 126.9 (dd, J_{CF} = 17.3, 17.2 Hz, Ar-C), 133.8 (dd, J_{CF} = 12.8, 12.6 Hz, Ar-C), 138.7 (Ar-C), 150.4 (Ar-C), 152.7 (dd, J_{CF} = 237.2, 9.0 Hz, Ar-C), 155.9 (Ar-C), 164.3 (C=O). HRMS cal. $C_{18}H_{22}F_2N_5O_2$ (ES+) m/z 378.174156 $[M+H]^+$, found 378.167664.

4.2.25 2-((3,5-Difluoro-4-hydroxyphenyl)amino)-8-isopentyl-5-methyl-7,8-dihydropteridin-6(5H)-one (34). Pteridinone heterocycle **22** (94 mg, 0.345 mmol), aniline **41** (102 mg, 0.689 mmol) and TFA (86 µL, 1.73 mmol) were taken up in TFE (3.5 mL) and reacted according to the described **General Procedure E**. Purification *via* silica gel chromatography (24:1 DCM:MeOH) and subsequent trituration with MeOH afforded the target compound as a white solid (64.4 mg, 0.17 mmol, 49%). Rf 0.39 (19:1 DCM:MeOH); M. p. 240-248°C decomposed; IR (cm^{-1}) 3281, 3096, 2960, 2916, 2872, 1649, 1618, 1562, 1524; ^{1}H NMR (400 MHz, DMSO-d_6) 0.93 (3H, d, J = 6.5 Hz, CH(CH_3)$_2$), 1.44-1.57 (2H, m, NCH$_2$CH_2), 1.57-1.70 (1H, m, CH(CH$_3$)$_2$), 3.20 (3H, s, NCH$_3$), 3.49-3.60 (2H, m, NCH_2CH$_2$), 4.15 (2H, s, NCH_2CO), 7.43 (2H, d, J = 10.7 Hz, H-2'/6'), 7.73 (1H, s, H-4), 9.07 (1H, s, NH), 9.38 (1H, s, OH); ^{13}C NMR (100 MHz, DMSO-d_6) 22.5 (CH(CH$_3$)$_2$), 22.9 (CH(CH$_3$)$_2$), 26.2 (CH(CH$_3$)$_2$), 27.8 (NCH$_3$),

4.2.26 2-((3-Fluoro-4-hydroxyphenyl)amino)-8-isopentyl-7,8-dihydropteridin-6(5H)-one (35). Pteridinone heterocycle **19** (75 mg, 0.294 mmol), 4-Amino-2-fluorophenol (78 mg, 0.59 mmol) and TFA (112 µL, 1.47 mmol) were taken up in TFE (3 mL) and reacted according to the described **General Procedure E**. Purification *via* silica gel chromatography (93:7 DCM:MeOH) and subsequent trituration with MeOH afforded the target compound as a purple solid (85 mg, 0.25 mmol, 83%). Rf 0.33 (93:7 DCM:MeOH); M. p. 210-247°C decomposed; IR (cm^{-1}) 3290, 2954, 1678, 1621, 1581, 1503; ^{1}H NMR (400 MHz, DMSO-d_6) 0.93 (6H, d, J = 6.6 Hz, CH(CH_3)$_2$), 1.44-1.70 (3H, m, CH(CH$_3$)$_2$, NCH$_2$CH_2), 3.52 (2H, t, J = 7.9 Hz, NCH_2CH$_2$), 4.04 (2H, s, NCH_2CO), 6.78 (1H, dd, J = 9.9, 9.0 Hz, H-5'), 7.14-7.22 (1H, m, H-6'), 7.46 (1H, s, H-4), 7.65 (1H, dd, J = 14.3, 2.4 Hz, H-2'), 8.80 (1H, s, NH), 9.20 (1H, s, OH), 10.37 (1H, s, NHCOCH$_2$); ^{13}C NMR (100 MHz, DMSO-d_6) 22.9 (CH(CH$_3$)$_2$), 26.3 (CH(CH$_3$)$_2$), 34.2 (NCH$_2C$H$_2$), 45.1 (NCH$_2$CH$_2$), 50.4 (NCH$_2$CO), 106.8 (d, J_{CF} = 23.1 Hz, Ar-C), 112.4 (Ar-C), 114.6 (d, J_{CF} = 2.8 Hz, Ar-C), 117.8 (d, J_{CF} = 3.9 Hz, Ar-C), 134.4 (d, J_{CF} = 9.5 Hz, Ar-C), 138.5 (d, J_{CF} = 3.3 Hz, Ar-C), 138.6 (Ar-C), 150.6 (Ar-C), 152.1 (d, J_{CF} = 237.5 Hz, Ar-C), 156.1 (Ar-C), 162.4 (C=O). HRMS cal. $C_{17}H_{21}FN_5O_2$ (ES+) m/z 346.167927 $[M+H]^+$, found 346.162472.

4.2.27 2-((3,5-Difluoro-4-hydroxyphenyl)amino)-8-isopentyl-7,8-dihydropteridin-6(5H)-one (**36**). Pteridinone heterocycle **19** (77 mg, 0.29 mmol), aniline **41** (87 mg, 0.59 mmol) and TFA (112 µL, 1.47 mmol) were taken up in TFE (3 mL) and reacted according to the described **General Procedure E**. Purification *via* silica gel chromatography (93:7 DCM:MeOH) and subsequent trituration with MeOH afforded the target compound as a brown solid (73 mg, 0.20 mmol, 67%). Rf 0.2 (1:2 Hexanes:EtOAc); M. p. 222-262°C decomposed; IR (cm^{-1}) 3294, 3114, 2956, 2869, 1681, 1621, 1583, 1517; ^{1}H NMR (400 MHz, DMSO-d_6) 0.93 (6H, d, J = 6.6 Hz, CH(CH_3)$_2$), 1.42-1.70 (3H, m, CH(CH$_3$)$_2$, NCH$_2$CH_2), 3.52 (2H, t, J = 7.9 Hz, NCH_2CH$_2$), 4.06 (2H, s, NCH_2CO), 7.41 (2H, d, J = 10.7 Hz, H-2'/6'), 7.48 (1H, s, H-4), 8.99 (1H, s, NH), 9.39 (1H, s, OH), 10.41 (1H, s, NHCOCH$_2$); ^{13}C NMR (100 MHz, DMSO-d_6) 22.9 (CH(CH$_3$)$_2$), 26.2 (CH(CH$_3$)$_2$), 34.2 (NCH$_2C$H$_2$), 45.2 (NCH$_2$CH$_2$), 50.4 (NCH$_2$CO), 101.7 (d, J_{CF} = 27.3 Hz, Ar-C), 112.9 (Ar-C), 126.9 (dd, J_{CF} = 16.7, 16.7 Hz, Ar-C), 133.8 (dd, J_{CF} = 12.8, 12.5 Hz, Ar-C), 138.3 (Ar-C), 150.5 (Ar-C), 152.7 (dd, J_{CF} = 237.5, 9.9 Hz, Ar-C), 155.7 (Ar-C), 162.4 (C=O). HRMS cal. $C_{17}H_{20}F_2N_5O_2$ (ES+) m/z 364.158506 $[M+H]^+$, found 364.150723.

4.2.28 2-((3-Fluoro-4-hydroxyphenyl)amino)-8-isopentyl-5-methyl-7,8-dihydropteridin-6(5H)-one (**37**). Pteridinone heterocycle **22** (75 mg, 0.28 mmol), 4-Amino-2-fluorophenol (75 mg, 0.56 mmol) and TFA (107 µL, 1.4 mmol) were taken up in TFE (3 mL) and reacted according to the described **General Procedure E**. Purification *via* silica gel chromatography (19:1 DCM:MeOH) and subsequent trituration with MeOH afforded the target compound as a purple solid (54.2 mg, 0.151 mmol, 54%). Rf 0.32 (19:1 DCM:MeOH); M. p. 247-252°C decomposed; IR (cm^{-1}) 3281, 2919, 1654, 1599; ^{1}H NMR (400 MHz, DMSO-d_6) 0.93 (6H, d, J = 6.5 Hz, CH(CH_3)$_2$), 1.45-1.56 (2H, m, NCH$_2$CH_2), 1.56-1.69 (1H, m, CH(CH$_3$)$_2$), 3.20 (3H, s, NCH_3), 3.53 (2H, t, J = 7.9 Hz, NCH_2CH$_2$), 4.13 (2H, s, NCH_2CO), 6.79 (1H, dd, J = 9.9,

9.3 [illegible] until 2'), 8.89 (1H, s, NH), 9.18 (1H, s, OH); ^{13}C NMR (100 MHz, DMSO-d_6) 22.9 (CH(CH_3)$_2$), 26.2 (CH(CH$_3$)$_2$), 27.7 (NCH$_3$), 34.2 (NCH$_2CH_2$), 45.1 (NCH_2CH$_2$), 50.3 (NCH_2CO), 106.9 (d, J_{CF} = 23.2 Hz, Ar-C), 114.6 (d, J_{CF} = 3.1 Hz, Ar-C), 114.7 (Ar-C), 117.8 (d, J_{CF} = 4.0 Hz, Ar-C), 134.3 (d, J_{CF} = 9.6 Hz, Ar-C), 138.6 (d, J_{CF} = 2.6 Hz, Ar-C), 138.7 (Ar-C), 150.8 (d, J_{CF} = 237.1 Hz, Ar-C), 151.2 (Ar-C), 156.0 (Ar-C), 161.3 (C=O). HRMS cal. $C_{18}H_{23}FN_5O_2$ (ES+) m/z 360.183578 [M+H]$^+$, found 360.179437.

4.2.29 2,6-Difluoro-4-(pyrimidin-2-ylamino)phenol (38). 2-Chloropyrimidine (32 mg, 0.262 mmol), aniline **41** (76 mg, 0.524 mmol) and TFA (100 µL, 1.31 mmol) were taken up in TFE (2.7 mL) and reacted according to the described **General Procedure E**. Purification by amine chromatography (1:1 DCM:MeOH) afforded the target compound as a brown solid (36.9 mg, 0.165 mmol, 63%). Rf 0.15 (1:1 DCM:MeOH); M. p. 200-203°C; IR (cm^{-1}) 3406, 2920, 2849, 1590, 1520; ^{1}H NMR (400 MHz, DMSO-d_6) 6.86 (1H, t, J = 4.8 Hz, H-5), 7.49 (2H, d, J = 10.9 Hz, H-3'/5'), 8.49 (2H, d, J = 4.8 Hz, H-4/6), 9.58 (1H, bs, OH), 9.67 (1H, s, NH); ^{13}C NMR (100 MHz, DMSO-d_6) 102.8 (d, J_{CF} = 27.1 Hz, Ar-C), 113.1 (Ar-C), 128.0 (dd, J_{CF} = 17.7, 15.2 Hz, Ar-C), 132.6 (dd, J_{CF} = 13.1, 12.5 Hz, Ar-C), 152.6 (dd, J_{CF} = 238.0, 8.9 Hz, Ar-C), 158.5 (Ar-C), 106.1 (Ar-C). HRMS cal. $C_{10}H_8F_2N_3O$ (ES+) m/z 224.063543 [M+H]$^+$, found 224.066029.

4.2.30 2-((3,5-Difluoro-4-hydroxyphenyl)amino)-5,7-dimethyl-7,8-dihydropteridin-6(5H)-one (39). Pteridinone heterocycle **23** (82 mg, 0.376 mmol), aniline **41** (110 mg, 0.752 mmol) and TFA (144 µL, 1.88 mmol) were taken up in TFE (4 mL) and reacted according to the described **General Procedure E**. Purification *via* silica gel chromatography (97:3 DCM:MeOH) and subsequent trituration with MeOH afforded the target compound as a brown solid (40 mg, 0.12 mmol, 32%). Rf 0.26 (1:2 Hexanes:EtOAc); M. p. 216-218°C; IR (cm^{-1}) 3455, 3420, 3330, 1661, 1608, 1522; ^{1}H NMR (400 MHz, DMSO-d_6) 1.36 (3H, d, J = 6.8 Hz, NHCHCH_3), 3.20 (3H, s, NCH$_3$), 4.20 (1H, q, J = 6.8 Hz, NHCHCH$_3$), 7.49 (2H, d, J = 11.0 Hz, H-2'/6'), 7.77 (2H, m, H-4, NHCHCH$_3$), 9.03 (1H, s, NH), 9.35 (1H, s, OH); ^{13}C NMR (100 MHz, DMSO-d_6) 20.2 (NCHCH_3), 28.2 (NCH$_3$), 51.1 (NCHCH$_3$), 101.9 (d, J_{CF} = 27.9 Hz, Ar-C), 114.8 (Ar-C), 126.9 (dd, J_{CF} = 17.3, 16.9 Hz, Ar-C), 133.8 (dd, J_{CF} = 12.9, 12.8 Hz, Ar-C),133.8 (Ar-C), 152.1 (Ar-C), 152.7 (dd, J_{CF} = 238.0., 9.2 Hz, Ar-C), 155.8 (Ar-C), 165.0 (C=O). HRMS cal. $C_{14}H_{14}F_2N_5O_2$ (ES+) m/z 322.111556 [M+H]$^+$, found 322.103014.

4.2.31 2-Chloro-5-nitropyrimidin-4-amine (40). A solution of 2,4-dichloro-5-nitropyrimidine (**14**) (0.90 g, 4.64 mmol) in DCM (6.7 mL, 0.7 M) was added dropwise to a solution of 2M Ammonia in EtOH (6 mL) stirring at 0°C. The reaction was stirred for 30 min at 0°C, after which the mixture was warmed to RT and the solvent removed *in vacuo*.[40] The crude residue was purified *via* silica gel chromatography (4:1 Hexanes:EtOAc) to afford the desired compound as a yellow solid (2.40 g, 13.8 mmol, 89%). Rf 0.24 (4:1 Hexanes:EtOAc); M.p. 212-213°C (Lit. = 220-221)[41]; IR (cm^{-1}) 3430, 3056, 1642, 1579, 1534; ^{1}H NMR (400 MHz, DMSO-d_6) 8.58 (1H, s, NH_2), 9.02 (1H, s, H-6), 9.19 (1H, s, NH_2); ^{13}C NMR (100 MHz, DMSO-d_6) δ 127.0 (Ar-C), 157.5 (Ar-C), 158.0 (Ar-C), 162.6 (Ar-C); HRMS cal. $C_4H_2ClN_4O_2$ (ES-) m/z 172.986629 [M-H]$^-$, found 172.988897.

4.2.32 4-Amino-2,6-difluorophenol (41). To a solution of 2,6-difluoro-4-nitrophenol (50 mg, 0.29 mmol) in EtOH (3 mL, 0.1 M) was added tin(II) chloride (0.22 g, 1.14 mmol). The reaction was heated under reflux for 1.5 h before the solvent was removed *in vacuo*. The resulting residue was dissolved in EtOAc:THF (1:1, 15 the aqueous phase reached pH 9-10. The resulting precipitate was removed *via* filtration and the organic extracts were collected, washed with brine (20 mL), evaporated to dryness, and purified *via* silica gel chromatography (19:1 DCM:MeOH) to afford the desired compound as a brown solid (0.37 g, 2.56 mmol, 77%). Rf 0.4 (19:1 DCM:MeOH); M.p. 140-150°C decomposed; IR (cm^{-1}) 3376, 3311, 2532, 1618, 1598, 1520; ^{1}H NMR (400 MHz, DMSO-d_6) 5.03 (2H, s, NH$_2$), 6.13-6.24 (2H, d, J = 9.9 Hz, H-3/5), 8.65 (1H, s, OH). ^{13}C NMR (100 MHz, DMSO-d_6) 97.7 (d, J_{CF} = 25.0 Hz, Ar-C), 123.3 (dd, J_{CF} = 17.1, 16.5 Hz, Ar-C), 142.1 (dd, J_{CF} = 12.8, 12.4 Hz, Ar-C), 154.0 (dd, J_{CF} = 238.1, 9.1 Hz, Ar-C). HRMS cal. $C_6H_4F_2NO$ (ES-) m/z 144.026095 [M-H]$^-$, found 144.027107.

4.2.33 4-Amino-2,6-dibromophenol (42). To a solution of 2,6-dibromo-4-nitrophenol (0.41 g, 1.35 mmol) in EtOH (13.5 mL, 0.1M) was added $SnCl_2$ (1.32 g, 6.74 mmol). The solution was heated under reflux for 1 h before the solvent was removed *in vacuo*. The sample was resuspended in EtOAc (1:1, 20 mL) and saturated $NaHCO_3$ solution was added until the aqueous phase reached a pH 9-10. The resulting precipitate was removed *via* filtration and the organic extracts were collected, washed with brine (30 mL), evaporated to dryness, and purified *via* silica gel chromatography (1:1 Hexanes:EtOAc) to afford the desired compound as a yellow solid (0.31 g, 1.16 mmol, 85%). Rf 0.69 (19:1 DCM:MeOH); M. p. 175-188°C decomposed; IR (cm^{-1}) 3365, 3265, 3158, 1602, 1561; ^{1}H NMR (400 MHz, DMSO-d_6) 5.01 (2H, s, NH$_2$), 6.76 (2H, s, H-3/5), 8.70 (1H, s, OH); ^{13}C NMR (100 MHz, DMSO-d_6) 114.0 (Ar-C), 117.6 (Ar-C), 140.9 (Ar-C), 144.7 (Ar-C). HRMS cal. $C_6H_4Br_2NO$ (ES-) m/z 263.86596 [M-H]$^-$, found 263.86705.

4.2.34 4-((4-Amino-5-nitropyrimidin-2-yl)amino)-2,6-difluorophenol (43). Pyrimidine **40** (71 mg, 0.396 mmol), aniline **41** (115 mg, 0.792 mmol) and TFA (152 µL, 1.98 mmol) were taken up in TFE (4 mL) and reacted according to the described **General Procedure E**. The crude material was resuspended in THF (20 mL), filtered over Celite, and the filtrate was concentrated *in vacuo*. Trituration of the crude material with MeOH afforded the target compound as a brown solid (66 mg, 0.23 mmol, 58%). Rf 0.47 (9:1 DCM:MeOH); M. p. 253-277°C decomposed; IR (cm^{-1}) 3481, 3375, 3251, 1628, 1599, 1552, 1521; ^{1}H NMR (400 MHz, DMSO-d_6) 7.49-7.77 (2H, m, H-3'/5'), 8.24 (1H, bs, NH$_2$), 8.74 (1H, bs, NH$_2$), 8.97 (1H, s, H-4), 9.80 (1H, s, NH), 10.24 (1H, bs, OH); ^{13}C NMR (100 MHz, DMSO-d_6) 104.1 (d, J_{CF} = 27.2 Hz, Ar-C), 129.4 (dd, J_{CF} = 16.8, 16.6 Hz, Ar-C), 131.2 (dd, J_{CF} = 12.6, 12.6 Hz, Ar-C), 152.5 (dd, J_{CF} = 238.2, 8.9 Hz, Ar-C), 157.6 (Ar-C), 157.7 (Ar-C), 159.8 (Ar-C). HRMS cal. $C_{10}H_8F_2N_5O_3$ (ES+) m/z 284.059521 [M+H]$^+$, found 284.06317.

4.2.35 4-((4,5-Diaminopyrimidin-2-yl)amino)-2,6-difluorophenol (44). To a solution of 5-nitropyrimidine **43** (58.7 mg, 0.205 mmol, 1 equiv.) in EtOH (2.5 mL, 0.1M) was added tin (II) chloride (159 mg, 0.82 mmol, 4 equiv.). The reaction was heated at reflux for 24 h before the reaction was cooled to RT and concentrated *in vacuo*. The sample was resuspended in EtOAc:THF (1:1, 20 mL) and a saturated aqueous solution of $NaHCO_3$ was added until the aqueous phase reached pH 9-10. The resulting precipitate was removed *via* filtration and the organic phase was collected, washed with brine (20 mL), dried ($MgSO_4$), and concentrated *in vacuo*. The crude residue was purified by silica gel chromatography (1:1 DCM:MeOH) to give the desired compound as a brown solid (21.1 mg, 0.083 mmol, 41%). Rf 0.11 (9:1 DCM:MeOH); M. p. 218-227°C decomposed; IR (cm^{-1}) 3442, 3208, 1641, 1580, 1523; ^{1}H NMR (400 MHz, DMSO-d_6) 4.20 (2H, s, NH$_2$), 6.29 (2H, s, NH$_2$), 7.40 (1H, s, H-4), 7.44 (2H, d, J = 11.1

Hz, d *in* MHz, DMSO-d_6) 100.9 (d, J_{CF} = 27.3 Hz, Ar-C), 120.9 (Ar-C), 125.9 (Ar-C), 134.9 (dd, J_{CF} = 12.8, 12.3 Hz, Ar-C), 138.3 (dd, J_{CF} = 17.7, 13.2 Hz, Ar-C), 152.8 (dd, J_{CF} = 227.6, 8.9 Hz, Ar-C), 153.0 (Ar-C), 155.2 (Ar-C), 156.4 (Ar-C). HRMS cal. $C_{10}H_{10}F_2N_5O$ (ES+) m/z 254.085341 $[M+H]^+$, found 254.086226.

4.2.36 Triisopropyl((4-nitrobenzyl)oxy)silane (45). To an oven dried flask cooled under N_2 was added a solution of benzyl alcohol (0.10 g, 0.65 mmol) in anhydrous DMF (1.3 mL, 0.5M). To the stirring solution was added imidazole (0.11 g, 1.63 mmol) followed by TIPS-Cl (168 µL, 0.78 mmol). The solution was stirred at RT for 2 h prior to neutralization with 2M HCl. The crude material was then extracted with DCM (3 x 15 mL), dried ($MgSO_4$), and the combined organic extracts were concentrated *in vacuo*. The crude material was purified *via* silica gel chromatography (19:1 Hexanes:EtOAc) to afford the desired compound as a colorless oil (0.59 g, 1.92 mmol, 95% yield). Rf 0.58 (9:1 Hexanes:EtOAc); IR (cm^{-1}) 2942, 2864, 1603, 1520; ^{1}H NMR (400 MHz, DMSO-d_6) 1.06 (18H, d, J = 7.1 Hz, Si(CH(CH_3)$_2$)$_3$), 1.12-1.16 (3H, m, Si(CH(CH$_3$)$_2$)$_3$), 4.95 (2H, s, OCH_2), 7.62 (2H, d, J = 8.4 Hz, H-2/6), 8.24 (2H, d, J = 8.4 Hz, H-3/5). ^{13}C NMR (100 MHz, DMSO-d_6) 11.8 (Si(CH(CH$_3$)$_2$), 18.3 (Si(CH(CH_3)$_2$), 64.2 (benzyl-CH$_2$), 123.9 (Ar-C), 127.0 (Ar-C), 146.9 (Ar-C), 149.8 (Ar-C). HRMS cal. $C_{16}H_{28}NO_3Si$ (ES+) m/z 310.183847 $[M+H]^+$, found 310.189782.

4.2.37 Triisopropyl(4-nitrophenoxy)silane (46). To an oven dried flask cooled under N_2 was added a solution of nitrophenol (0.11 g, 0.72 mmol) in anhydrous DMF (1.5 mL, 0.5M). To the stirring solution was added imidazole (0.12 g, 1.80 mmol) followed by TIPS-Cl (185 ul, 0.86 mmol). The solution was stirred at RT for 2 h prior to neutralization with 2M HCl. The crude material was then extracted with DCM (3 x 15 mL), dried ($MgSO_4$), and the combined organic extracts were concentrated *in vacuo*. The crude material was purified *via* silica gel chromatography (19:1 Hexanes:EtOAc) to afford the desired compound as a colorless oil (0.60 g, 2.02 mmol, 90% yield). Rf 0.63 (9:1 Hexanes:EtOAc); IR (cm^{-1}) 2945, 2866, 1682, 1590; ^{1}H NMR (400 MHz, DMSO-d_6) 1.07 (18H, d, J = 7.5 Hz, Si(CH(CH_3)$_2$)$_3$), 1.32 (3H, m, Si(CH(CH$_3$)$_2$)$_3$), 7.07 (2H, d, J = 9.1 Hz, H-2/6), 8.18 (2H, d, J = 9.1 Hz, H-3/5). ^{13}C NMR (100 MHz, DMSO-d_6) 12.5 (Si(CH(CH$_3$)$_2$), 18.3 (Si(CH(CH_3)$_2$), 116.3 (Ar-C), 126.6 (Ar-C), 140.1 (Ar-C), 164.4 (Ar-C). HRMS cal. $C_{15}H_{26}NO_3Si$ (ES+) m/z 296.168197 $[M+H]^+$, found 296.170894.

4.2.38 4-(((Triisopropylsilyl)oxy)methyl)aniline (47). A solution of nitrobenzyl alcohol **45** (0.58 g, 1.84 mmol) and Pd/C (60.4 mg, 10% w/w) in EtOH (18 mL, 0.1M) was hydrogenated for 3 h prior to filtration of the palladium. The filtrate was concentrated *in vacuo* and the crude residue was purified *via* silica gel chromatography (4:1 Hexanes:EtOAc) to afford the desired compound as a colorless oil (0.43 g, 1.54 mmol, 83%). Rf 0.22 (9:1 Hexanes:EtOAc); IR (cm^{-1}) 3447, 3363, 2939, 2862, 1622, 1516; ^{1}H NMR (400 MHz, DMSO-d_6) 0.91-1.21 (3H, m, Si(CH(CH$_3$)$_2$)$_3$), 1.03 (18H, d, J = 6.4 Hz, Si(CH(CH_3)$_2$)$_3$), 4.59 (2H, s, OCH_2), 4.93 (2H, s, NH$_2$), 6.51 (2H, d, J = 8.2 Hz, H-2/6), 6.97 (2H, d, J = 8.2 Hz, H-3/5); ^{13}C NMR (100 MHz, DMSO-d_6) 12.0 (Si(CH(CH$_3$)$_2$), 18.4 (Si(CH(CH_3)$_2$), 65.2 (benzyl-CH$_2$), 114.1 (Ar-C), 127.7 (Ar-C), 128.8 (Ar-C), 148.1 (Ar-C). HRMS cal. $C_{16}H_{30}NOSi$ (ES+) m/z 280.209666 $[M+H]^+$, found 280.208982.

4.2.39 4-((Triisopropylsilyl)oxy)aniline (48). A solution of TIPS-protected nitrophenol **46** (0.58 g, 1.96 mmol) and Pd/C (64.2 mg, 10% w/w) in EtOH (19 mL, 0.1M) was hydrogenated for 3 h *in vacuo* and the crude residue was purified *via* silica gel chromatography (4:1 Hexanes:EtOAc) to afford the desired compound as a colorless oil (0.50 g, 1.87 mmol, 95%). Rf 0.25 (4:1 Hexanes:EtOAc); IR (cm^{-1}) 3430, 3351, 2941, 2864, 1615, 1505; ^{1}H NMR (400 MHz, DMSO-d_6) 1.04 (18H, d, J = 7.1 Hz, Si(CH(CH_3)$_2$)$_3$), 1.11- 1.26 (3H, m, Si(CH(CH$_3$)$_2$)$_3$), 4.59 (2H, s, NH$_2$), 6.45 (2H, d, J = 8.7 Hz, H-2/6), 6.56 (2H, d, J = 8.7 Hz, H-3/5); ^{13}C NMR (100 MHz, DMSO-d_6) 12.5 (Si(CH(CH$_3$)$_2$), 18.0 (Si(CH(CH_3)$_2$), 115.4 (Ar-C), 120.2 (Ar-C), 143.1 (Ar-C), 146.4 (Ar-C).
HRMS cal. $C_{15}H_{28}NOSi$ (ES+) m/z 266.194017 $[M+H]^+$, found 266.187327.

4.2.40 8-Isopentyl-5,7-dimethyl-2-((4-(((triisopropylsilyl)oxy)methyl)phenyl)amino)-7,8-dihydropteridin-6(5H)-one (49). Pteridinone heterocycle **21** (81 mg, 0.28 mmol), TIPS-protected aniline **47** (96 mg, 0.057 mmol) and K_2CO_3 (103 mg, 0.71 mmol) were taken up in MeCN (3 mL 0.1M), degassed under a stream of N_2, and heated to 110°C for 2 h. The reaction was then cooled, filtered over Celite and the filtrate concentrated *in vacuo*. Purification *via* silica gel chromatography (1:2 Hexanes:EtOAc) afforded the desired compound as an impure yellow oil (46.7 mg, 0.09 mmol, 31%). Rf 0.32 (1:2 Hexanes:EtOAc). Crude product was taken through for deprotection as **26** without further characterization of intermediate **49**.

4.2.41 8-Isopentyl-5,7-dimethyl-2-((4-((triisopropylsilyl)oxy)phenyl)amino)-7,8-dihydropteridin-6(5H)-one (50). Pteridinone heterocycle **21** (81 mg, 0.28 mmol), TIPS-protected aniline **48** (92 mg, 0.34 mmol) and K_2CO_3 (103 mg, 0.71 mmol) were taken up in MeCN (3 mL, 0.1M), degassed under a stream of N_2, and heated to 110°C for 2 h. The reaction was then cooled, filtered over Celite and the filtrate concentrated *in vacuo*. Purification *via* silica gel chromatography (1:2 Hexanes:EtOAc) afforded the desired compound as an impure yellow oil (43.2 mg, 0.08 mmol, 30%). Crude product was taken through for deprotection as **27** without further characterization of intermediate **50**.

4.2.42 2-((3-Fluoro-4-methoxyphenyl)amino)-8-isopentyl-5,7-dimethyl-7,8-dihydropteridin-6(5H)-one (51). Pteridinone heterocycle **21** (120 mg, 0.42 mmol), monofluoro-methoxyaniline (124 mg, 0.85 mmol) and TFA (162 µL, 2.12 mmol) were taken up in TFE (4 mL) and reacted according to the described **General Procedure E**. Purification *via* silica gel chromatography (97:3 DCM:MeOH) afforded the target compound as a pink solid (0.15 g, 0.38 mmol, 89%). Rf 0.32 (97:3 DCM:MeOH); M. p. 135-173°C decomposed; IR (cm^{-1}) 3259, 2958, 1667, 1608, 1575, 1515; ^{1}H NMR (400 MHz, DMSO-d_6) 0.87 (3H, d, J = 6.4 Hz, CH(CH_3)$_2$), 0.89 (3H, d, J = 6.5 Hz, CH(CH_3)$_2$), 1.36 (3H, d, J = 6.8 Hz, NCHCH_3), 1.40-1.52 (1H, m, CH(CH$_3$)$_2$), 1.52-1.65 (2H, m, NCH$_2$CH_2), 3.14-3.27 (1H, m, NCH_2CH$_2$), 3.20 (1H, s, NCH$_3$), 3.80 (3H, s, OCH$_3$), 3.86-3.98 (1H, m, NCH_2CH$_2$), 4.36 (1H, q, J = 6.8 Hz, NCHCH$_3$), 7.09 (1H, dd, J = 9.3, 9.3 Hz, H-5'), 7.21-7.29 (1H, m, H-6'), 7.64 (1H, dd, J = 13.9, 2.4 Hz, H-2'), 7.73 (1H, s, H-4), 9.68 (1H, s, NH); ^{13}C NMR (100 MHz, DMSO-d_6) 18.3 (NCHCH$_3$), 22.7 (CH(CH_3)$_2$), 22.8 (CH(CH_3)$_2$), 26.2 (CH(CH$_3$)$_2$), 28.4 (NCH$_3$), 35.7 (NCH$_2$CH_2), 44.4 (NCH_2CH$_2$), 56.7, 56.8, 108.9 (d, J_{CF} = 23.1 Hz, Ar-C), 114.6 (d, J_{CF} = 2.5 Hz, Ar-C), 115.3 (Ar-C), 116.5 (Ar-C), 133.3 (d, J_{CF} = 9.8 Hz, Ar-C), 143.0 (d, J_{CF} = 10.3 Hz, Ar-C), 150.3 (Ar-C), 151.5 (Ar-C), 152.7 (Ar-C), 152.9 (Ar-C), 164.0 (C=O). HRMS cal. $C_{20}H_{27}FN_5O_2$ (ES+) m/z 388.214878 $[M+H]^+$, found 388.210712.

4.2.43 2-((3-Chloro-4-methoxyphenyl)amino)-8-isopentyl-5,7-dimethyl-7,8-dihydropteridin-6(5H)-one (52). Pteridinone heterocycle **21** (123 mg, 0.42 mmol), monochloro-methoxyaniline (138 mg, 0.85 mmol) and TFA (162 µL, 2.12 mmol) were taken up in TFE (4 mL) and reacted according to the described **General Procedure E**. Purification *via* silica gel chromatography (49:1 DCM:MeOH) afforded the target compound as a brown solid (0.13 g, 0.33 mmol, 76%). Rf 0.38 (97:3 DCM:MeOH); M. p. 173-188°C decomposed; IR (cm^{-1}) 2948, 1669, 1606; ^1H NMR (400 MHz, DMSO-d_6) 0.84 (3H, d, J = 5.9 Hz, $CH(CH_3)_2$), 0.86 (3H, d, J = 5.9 Hz, $CH(CH_3)_2$), 1.34-1.49 (1H, m, $CH(CH_3)_2$), 1.39 (3H, d, J = 6.8 Hz, $NCHCH_3$), 1.49-1.63 (2H, m, NCH_2CH_2), 3.17-3.28 (1H, m, NCH_2CH_2), 3.20 (3H, s, NCH_3), 3.78-3.95 (1H, m, NCH_2CH_2), 3.83 (3H, s, OCH_3), 4.39 (1H, q, J = 6.8 Hz, $NCHCH_3$), 7.12 (1H, d, J = 8.9 Hz, H-5'), 7.41 (1H, dd, J = 8.9, 2.4 Hz, H-6'), 7.72 (1H, s, H-4), 7.74 (1H, d, J = 2.4 Hz, H-2'), 9.93 (1H, s, NH); ^{13}C NMR (100 MHz, DMSO-d_6) 18.8 ($NCHCH_3$), 22.7 ($CH(CH_3)_2$), 22.8 ($CH(CH_3)_2$), 26.2 ($CH(CH_3)_2$), 28.6 (NCH_3), 35.5 (NCH_2CH_2), 45.0 (NCH_2CH_2), 56.7, 56.9, 113.4 (Ar-C), 115.5 (Ar-C), 121.3 (Ar-C), 121.7 (Ar-C), 123.4 (Ar-C), 132.1 (Ar-C), 151.1 (Ar-C), 151.6 (Ar-C), 151.8 (Ar-C), 163.9 (C=O). HRMS cal. $C_{20}H_{27}ClN_5O_2$ (ES+) m/z 404.185328 $[M+H]^+$, found 404.178289.

4.2.44 2-((3-Bromo-4-methoxyphenyl)amino)-8-isopentyl-5,7-dimethyl-7,8-dihydropteridin-6(5H)-one (53). Pteridinone heterocycle **21** (123 mg, 0.42 mmol), monobromo-methoxyaniline (174 mg, 0.85 mmol) and TFA (162 µL, 2.12 mmol) were taken up in TFE (4 mL) and reacted according to the described **General Procedure E**. Purification *via* silica gel chromatography (97:3 DCM:MeOH) afforded the target compound as a purple solid (0.19 g, 0.43 mmol, 98%). Rf 0.28 (97:3 DCM:MeOH); M. p. 143-158°C decomposed; IR (cm^{-1}) 2962, 1674, 1565, 1528; ^1H NMR (400 MHz, DMSO-d_6) 0.84 (3H, d, J = 5.9 Hz, $CH(CH_3)_2$), 0.86 (3H, d, J = 5.9 Hz, $CH(CH_3)_2$), 1.35-1.49 (1H, m, $CH(CH_3)_2$), 1.39 (3H, d, J = 6.8 Hz, $NCHCH_3$), 1.49-1.63 (2H, m, NCH_2CH_2), 3.15-3.29 (1H, m, NCH_2CH_2), 3.20 (1H, s, NCH_3), 3.82 (3H, s, OCH_3), 3.85-3.95 (1H, m, NCH_2CH_2), 4.40 (1H, q, J = 6.8 Hz, $NCHCH_3$), 7.09 (1H, d, J = 8.9 Hz, H-5'), 7.45 (1H, dd, J = 8.9, 2.5 Hz, H-6'), 7.71 (1H, s, H-4), 7.88 (1H, d, J = 2.5 Hz, H-2'), 9.96 (1H, s, NH); ^{13}C NMR (100 MHz, DMSO-d_6) 18.7 ($NCHCH_3$), 22.7 ($CH(CH_3)_2$), 22.8 ($CH(CH_3)_2$), 26.2 ($CH(CH_3)_2$), 28.6 (NCH_3), 35.5 (NCH_2CH_2), 44.8 (NCH_2CH_2), 56.8, 56.9, 110.7 (Ar-C), 113.2 (Ar-C), 115.5 (Ar-C), 122.4 (Ar-C), 126.4 (Ar-C), 132.6 (Ar-C), 151.5 (Ar-C), 151.8 (Ar-C), 152.4 (Ar-C), 163.9 (C=O). HRMS cal. $C_{20}H_{27}BrN_5O_2$ (ES+) m/z 448.134811 $[M+H]^+$, found 448.131605.

4.3 Inhibition of RSK activity

LANCE (Lanthanide Chelate Excite)® Eu time-resolved fluorescence resonance energy transfer (TR-FRET) kinase assay (PerkinElmer) was performed in 384-well OptiPlates (Corning) using recombinant RSK1, RSK2, RSK3 and RSK4 kinases (CarnaBio), ULight™-phospho-40S ribosomal protein S6 (Ser235/236) peptide substrate (PerkinElmer), and ATP (Sigma) according to the supplier protocols. All reagents were prepared in kinase buffer containing 2mM DTT, 50 mM HEPES, 1mM EGTA, 10 mM $MgCl_2$, 0.01% Tween 20, pH 7.5. Inhibitor solutions were prepared such that the final DMSO concentration did not exceed 0.5%, which was shown to have no impact on kinase activity. RSK1 was used at a final concentration of 1 nM while RSK2, RSK3 and RSK4 were used at a final concentration of 500 pM. ULight™-rpS6 substrate was used at a final concentration of 250 nM for all isoforms and ATP was administered at a final concentration of 5 µM, 3 µM, 1 µM and 6 µM for RSK1, RSK2, RSK3 and RSK4 respectively. Solutions were prepared in a reaction mixture consisting of 2 µL serially diluted inhibitor solution, 4 µL kinase, 2 µL substrate, and 2 µL ATP. Reagents were incubated at room temperature for 1 h before the reaction was stopped through the addition of 5 µL of EDTA at a final concentration of 10 mM. After a 5 min incubation period, 5 µL of Eu anti-phospho-40S Ribosomal Protein S6 (Ser235/236) antibody (PerkinElmer) at a final concentration of 2 nM was added. The plate was read using a Biotek Synergy H1 Hybrid plate reader (Excitation=340 nm; Substrate emission=665 nm; Antibody emission=615 nm; Delay=100 µs; Integration=200 µs). Emission ratios (665 nm/615 nm) were calculated for each well and half-maximal inhibitory concentrations (IC_{50}) were determined for each inhibitor through non-linear regression analysis of the log dose-response curves.

4.4 Cell culture

MOLM-13 (DSMZ), MOLM-14 (DSMZ), THP-1 (ATCC), and U937 cells were cultured in RPMI1640 (Gibco) supplemented with 10% FBS (Sigma Aldrich) and 1% penicillin/streptomycin solution (Cellgro), K562 and MV4-11 were cultured in Iscove Modified Dulbecco Medium (IMDM; Gibco) supplemented with 10% FBS (Sigma Aldrich) and 1% penicillin/streptomycin solution (Cellgro), and HL-60 cells were cultured in Iscove Modified Dulbecco Medium (IMDM; Gibco) supplemented with 20% FBS (Sigma Aldrich) and 1% penicillin/streptomycin solution (Cellgro) at 37°C in an incubator humidifier with 95% air and 5% CO_2. HEK293 cells (ATCC) were cultured in Dulbecco's Modified Eagle Medium (DMEM; Gibco) supplemented with 10% FBS (Sigma Aldrich) and 1% penicillin/streptomycin solution (Cellgro) at 37°C in an incubator humidifier with 95% air and 5% CO_2. HEK293 cells were allowed to adhere for 24 h prior to use in assays. In all assays, the final DMSO concentration did not exceed 0.5% for all treatment conditions.

4.5 Western blot

Cell lines were maintained according to cell culture protocol prior to preparation of untreated cell lysates for Western blot analysis. Cells were trypsinized (if adherent), collected and centrifuged at 1000 rpm for 10 minutes at 4°C. Media was aspirated and cells were washed with phosphate buffered saline (PBS) and centrifuged again. PBS was aspirated and cell pellets were resuspended in TES/SB buffer supplemented with protease inhibitors and kept on ice for the duration of lysate preparation. Samples were sonicated (3 x 5 s) and centrifuged at 12000 rpm for 10 minutes at 4°C. Protein concentrations of isolated lysates were determined for each cell line via a Lowry Protein Assay (according to supplier protocol) and diluted such that each sample contains 25 µg of total protein in 40 µL of TES/SB buffer supplemented with SDS Loading Buffer and 20% BME. Lysates were centrifuged and boiled for 10 minutes prior to loading into a 10% acrylamide gel. The gel was run and the proteins transferred to a nitrocellulose membrane, blocked with 5% milk in TBS-T for 1 h, and incubated with the necessary primary antibody at the indicated dilution in TBS-T containing 5% BSA overnight at 4°C. Membranes were washed in TBS-T, and incubated with the appropriate secondary antibody for 45 minutes. Gels were developed on a Biorad ChemiDoc™ MP Imaging System according to the manufacturer's protocol. Antibodies used included phosphor-RSK1(Ser221), total-RSK1, phosphor-RSK2 (Ser227), and total-RSK2 and were purchased from Cell Signaling Technologies.

4.6 Cellular Metabolic Viability and Cytotoxicity Assays.

4.6. [illegible] seeded into sterile 96-well plates (Corning) at 60,000 cells per well in 100 µL of media. Inhibitor solutions were administered in 50 µL over a concentration range from 60 µM to 247 nM and cells were incubated at 37°C for 24 to 72 h. Following 3 h incubation with 30 µL CellTiter 96® Aqueous One Cell Proliferation Reagent (Promega), cell viability was measured by formazan concentration assessment through colorimetric analysis using a Biotek Synergy H1 Hybrid plate reader (Absorption=490).

4.6.2 CellTiter-Glo Viability Assay. MOLM-13 cells were seeded into sterile opaque 96-well plates (Thermo Scientific) at 30,000 cells per well in 50 µL of media. Inhibitor solutions were administered in 50 µL over a concentration range from 60 µM to 247 nM and cells were incubated at 37°C for 24 to 72 h. Cells were equilibrated at RT for 30 min, dosed with 100 µL CellTiter-Glo® Reagent, and mixed on an orbital shaker for 2 min. Luminescence was measured following 10 min incubation at rt using a BioTek Synergy H1 plate reader.

4.6.3 CellTox Green Cytotoxicity Assay. MOLM-13 cells were seeded into sterile black 96-well plates (Corning) at 60,000 cells per well in 50 µL of media containing 1:500 dilution of CellTox™ Green dye (Promega). Inhibitor solutions were administered in 50 µL over a concentration range from 60 µM to 247 nM. Cells were incubated at 37˚C and fluorescence was measured at 0, 24, 48 and 72 h using a BioTek Synergy H1 plate reader (Excitation=485 nm; Emission=520 nm).

4.7 Intracellular RSK2 Kinase Assay

HEK293 cells were cultured in DMEM, as indicated above, prior to transfection. Cells were pelleted and resuspended in DMEM to a density of 200,000 cells per mL. A lipid:DNA complex containing a 9:1 ratio of Transfection Carrier DNA to NanoLuc®-RPS6KA3 fusion DNA was prepared according to Promega NanoBRET™ Intracellular Kinase Assay protocol (K-5 kit). A solution containing 1 part lipid:DNA complex with 20 parts HEK293 cells was dispensed into an appropriate sterile tissue culture flask such that a cell density of 55,000-80,000 cells per cm^2 is reached and incubated for 24 h. Following transfection, media was aspirated and cells were readjusted to a density of 200,000 cells per mL in Opti-MEM I Reduced Serum Medium (no phenol red; Gibco). Cell solution was administered at 85 µL per well into sterile white 96-well plates (Thermo Scientific). A 20X NanoBRET® Tracer K-5 reagent was prepared according to protocol and administered at 5 µL per well. Inhibitor solutions were administered in 10 µL over a concentration range from 40 µM to 1.25 µM and cells were incubated for 2 h at 37˚C. The plates were equilibrated at rt for 15 min prior to administration of 50 µL 3X Complete Substrate plus Extracellular Inhibitor solution containing Nano-Glo® Substrate and Extracellular NanoLuc® Inhibitor, prepared according to assay protocol. Cells were incubated at rt for 2-3 min and fluorescence was measured using a BioTek Synergy H1 plate reader (Donor = 450 nm; Acceptor = 610 nm). BRET ratios were calculated by dividing the acceptor emission by the donor emission, correcting for background by subtracting the 'no tracer' BRET ratio from each sample.

Acknowledgement

Research reported in this publication was supported by an ALSAM Therapeutics Innovation grant.

References and Notes

ses: emerging roles in cellular signalling. *Nat Rev Mol Cell Biol* **2008,** *9* (10), 747-58.
2. Romeo, Y.; Zhang, X.; Roux, P. P., Regulation and function of the RSK family of protein kinases. *Biochem J* **2012,** *441* (2), 553-69.
3. Lara, R.; Seckl, M. J.; Pardo, O. E., The p90 RSK family members: common functions and isoform specificity. *Cancer Res* **2013,** *73* (17), 5301-8.
4. Carriere, A.; Ray, H.; Blenis, J.; Roux, P. P., The RSK factors of activating the Ras/MAPK signaling cascade. *Front Biosci* **2008,** *13*, 4258-75.
5. Dummler, B. A.; Hauge, C.; Silber, J.; Yntema, H. G.; Kruse, L. S.; Kofoed, B.; Hemmings, B. A.; Alessi, D. R.; Frodin, M., Functional characterization of human RSK4, a new 90-kDa ribosomal S6 kinase, reveals constitutive activation in most cell types. *J Biol Chem* **2005,** *280* (14), 13304-14.
6. Richards, S. A.; Fu, J.; Romanelli, A.; Shimamura, A.; Blenis, J., Ribosomal S6 kinase 1 (RSK1) activation requires signals dependent on and independent of the MAP kinase ERK. *Curr Biol* **1999,** *9* (15), 810-20.
7. Romeo, Y.; Roux, P. P., Paving the way for targeting RSK in cancer. *Expert Opin Ther Targets* **2011,** *15* (1), 5-9.
8. Houles, T.; Roux, P. P., Defining the role of the RSK isoforms in cancer. *Semin Cancer Biol* **2018,** *48*, 53-61.
9. McCubrey, J. A.; Steelman, L. S.; Chappell, W. H.; Abrams, S. L.; Wong, E. W.; Chang, F.; Lehmann, B.; Terrian, D. M.; Milella, M.; Tafuri, A.; Stivala, F.; Libra, M.; Basecke, J.; Evangelisti, C.; Martelli, A. M.; Franklin, R. A., Roles of the Raf/MEK/ERK pathway in cell growth, malignant transformation and drug resistance. *Biochim Biophys Acta* **2007,** *1773* (8), 1263-84.
10. Steelman, L. S.; Franklin, R. A.; Abrams, S. L.; Chappell, W.; Kempf, C. R.; Basecke, J.; Stivala, F.; Donia, M.; Fagone, P.; Nicoletti, F.; Libra, M.; Ruvolo, P.; Ruvolo, V.; Evangelisti, C.; Martelli, A. M.; McCubrey, J. A., Roles of the Ras/Raf/MEK/ERK pathway in leukemia therapy. *Leukemia* **2011,** *25* (7), 1080-94.
11. Yang, X.; Liu, L.; Sternberg, D.; Tang, L.; Galinsky, I.; DeAngelo, D.; Stone, R., The FLT3 internal tandem duplication mutation prevents apoptosis in interleukin-3-deprived BaF3 cells due to protein kinase A and ribosomal S6 kinase 1-mediated BAD phosphorylation at serine 112. *Cancer Res* **2005,** *65* (16), 7338-47.
12. Elf, S.; Blevins, D.; Jin, L.; Chung, T. W.; Williams, I. R.; Lee, B. H.; Lin, J. X.; Leonard, W. J.; Taunton, J.; Khoury, H. J.; Kang, S., p90RSK2 is essential for FLT3-ITD- but dispensable for BCR-ABL-induced myeloid leukemia. *Blood* **2011,** *117* (25), 6885-94.
13. Kang, S.; Dong, S.; Gu, T. L.; Guo, A.; Cohen, M. S.; Lonial, S.; Khoury, H. J.; Fabbro, D.; Gilliland, D. G.; Bergsagel, P. L.; Taunton, J.; Polakiewicz, R. D.; Chen, J., FGFR3 activates RSK2 to mediate hematopoietic transformation through tyrosine phosphorylation of RSK2 and activation of the MEK/ERK pathway. *Cancer Cell* **2007,** *12* (3), 201-14.
14. Kang, S.; Elf, S.; Dong, S.; Hitosugi, T.; Lythgoe, K.; Guo, A.; Ruan, H.; Lonial, S.; Khoury, H. J.; Williams, I. R.; Lee, B. H.; Roesel, J. L.; Karsenty, G.; Hanauer, A.; Taunton, J.; Boggon, T. J.; Gu, T. L.; Chen, J., Fibroblast growth factor receptor 3 associates with and tyrosine phosphorylates p90 RSK2, leading to RSK2 activation that mediates hematopoietic transformation. *Mol Cell Biol* **2009,** *29* (8), 2105-17.
15. Mitton, B.; Dutta, R.; Hsu, Y.-C.; Sakamoto, K., The Role of pp90rsk-Mediated CREB Phosphorylation in Acute Myelogenous Leukemia. *Blood* **2014,** *124* (21), 2229-2229.

16. N.; leukemogenesis. *Crit Rev Oncog* **2011,** *16* (1-2), 37-46.
17. Bonni, A.; Brunet, A.; West, A. E.; Datta, S. R.; Takasu, M. A.; Greenberg, M. E., Cell survival promoted by the Ras-MAPK signaling pathway by transcription-dependent and -independent mechanisms. *Science* **1999,** *286* (5443), 1358-62.
18. Smith, J. A.; Maloney, D. J.; Hecht, S. M.; Lannigan, D. A., Structural basis for the activity of the RSK-specific inhibitor, SL0101. *Bioorg Med Chem* **2007,** *15* (14), 5018-34.
19. Hilinski, M. K.; Mrozowski, R. M.; Clark, D. E.; Lannigan, D. A., Analogs of the RSK inhibitor SL0101: optimization of in vitro biological stability. *Bioorg Med Chem Lett* **2012,** *22* (9), 3244-7.
20. Cohen, M. S.; Hadjivassiliou, H.; Taunton, J., A clickable inhibitor reveals context-dependent autoactivation of p90 RSK. *Nat Chem Biol* **2007,** *3* (3), 156-60.
21. Zaru, R.; Ronkina, N.; Gaestel, M.; Arthur, J. S.; Watts, C., The MAPK-activated kinase Rsk controls an acute Toll-like receptor signaling response in dendritic cells and is activated through two distinct pathways. *Nat Immunol* **2007,** *8* (11), 1227-35.
22. Sapkota, G. P.; Cummings, L.; Newell, F. S.; Armstrong, C.; Bain, J.; Frodin, M.; Grauert, M.; Hoffmann, M.; Schnapp, G.; Steegmaier, M.; Cohen, P.; Alessi, D. R., BI-D1870 is a specific inhibitor of the p90 RSK (ribosomal S6 kinase) isoforms in vitro and in vivo. *Biochem J* **2007,** *401* (1), 29-38.
23. Edgar, A. J.; Trost, M.; Watts, C.; Zaru, R., A combination of SILAC and nucleotide acyl phosphate labelling reveals unexpected targets of the Rsk inhibitor BI-D1870. *Biosci Rep* **2013**.
24. Bain, J.; Plater, L.; Elliott, M.; Shpiro, N.; Hastie, C. J.; McLauchlan, H.; Klevernic, I.; Arthur, J. S.; Alessi, D. R.; Cohen, P., The selectivity of protein kinase inhibitors: a further update. *Biochem J* **2007,** *408* (3), 297-315.
25. Pambid, M. R.; Berns, R.; Adomat, H. H.; Hu, K.; Triscott, J.; Maurer, N.; Zisman, N.; Ramaswamy, V.; Hawkins, C. E.; Taylor, M. D.; Dunham, C.; Guns, E.; Dunn, S. E., Overcoming resistance to Sonic Hedgehog inhibition by targeting p90 ribosomal S6 kinase in pediatric medulloblastoma. *Pediatr Blood Cancer* **2014,** *61* (1), 107-15.
26. Hammoud, L.; Adams, J. R.; Loch, A. J.; Marcellus, R. C.; Uehling, D. E.; Aman, A.; Fladd, C.; McKee, T. D.; Jo, C. E.; Al-Awar, R.; Egan, S. E.; Rossant, J., Identification of RSK and TTK as Modulators of Blood Vessel Morphogenesis Using an Embryonic Stem Cell-Based Vascular Differentiation Assay. *Stem Cell Reports* **2016**.
27. Aronchik, I.; Appleton, B. A.; Basham, S. E.; Crawford, K.; Del Rosario, M.; Doyle, L. V.; Estacio, W. F.; Lan, J.; Lindvall, M. K.; Luu, C. A.; Ornelas, E.; Venetsanakos, E.; Shafer, C. M.; Jefferson, A. B., Novel potent and selective inhibitors of p90 ribosomal S6 kinase reveal the heterogeneity of RSK function in MAPK-driven cancers. *Mol Cancer Res* **2014,** *12* (5), 803-12.
28. Jain, R.; Mathur, M.; Lan, J.; Costales, A.; Atallah, G.; Ramurthy, S.; Subramanian, S.; Setti, L.; Feucht, P.; Warne, B.; Doyle, L.; Basham, S.; Jefferson, A. B.; Lindvall, M.; Appleton, B. A.; Shafer, C. M., Discovery of Potent and Selective RSK Inhibitors as Biological Probes. *J Med Chem* **2015,** *58* (17), 6766-83.
29. Carbain, B.; Coxon, C. R.; Lebraud, H.; Elliott, K. J.; Matheson, C. J.; Meschini, E.; Roberts, A. R.; Turner, D. M.; Wong, C.; Cano, C.; Griffin, R. J.; Hardcastle, I. R.; Golding, B. T., Trifluoroacetic acid in 2,2,2-trifluoroethanol facilitates S(N)Ar reactions of heterocycles with arylamines. *Chemistry* **2014,** *20* (8), 2311-7.
30. Martins, V. R., Two widely used RSK inhibitors, BI-D1870 and SL0101, alter mTORC1 signaling in a RSK-independent manner. *Cell Signal* **2015,** *27* (8), 1630-42.
31. Ciceri, P.; Muller, S.; O'Mahony, A.; Fedorov, O.; Filippakopoulos, P.; Hunt, J. P.; Lasater, E. A.; Pallares, G.; Picaud, S.; Wells, C.; Martin, S.; Wodicka, L. M.; Shah, N. P.; Treiber, D. K.; Knapp, S., Dual kinase-bromodomain inhibitors for rationally designed polypharmacology. *Nat Chem Biol* **2014,** *10* (4), 305-12.
32. Galvin, J. P.; Altman, J. K.; Szilard, A.; Goussetis, D. J.; Vakana, E.; Sassano, A.; Platanias, L. C., Regulation of the kinase RSK1 by arsenic trioxide and generation of antileukemic responses. *Cancer Biol Ther* **2013,** *14* (5), 411-6.
33. Stratford, A. L.; Reipas, K.; Hu, K.; Fotovati, A.; Brough, R.; Frankum, J.; Takhar, M.; Watson, P.; Ashworth, A.; Lord, C. J.; Lasham, A.; Print, C. G.; Dunn, S. E., Targeting p90 ribosomal S6 kinase eliminates tumor-initiating cells by inactivating Y-box binding protein-1 in triple-negative breast cancers. *Stem Cells* **2012,** *30* (7), 1338-48.
34. Friesner, R. A.; Banks, J. L.; Murphy, R. B.; Halgren, T. A.; Klicic, J. J.; Mainz, D. T.; Repasky, M. P.; Knoll, E. H.; Shelley, M.; Perry, J. K.; Shaw, D. E.; Francis, P.; Shenkin, P. S., Glide: a new approach for rapid, accurate docking and scoring. 1. Method and assessment of docking accuracy. *J Med Chem* **2004,** *47* (7), 1739-49.
35. Friesner, R. A.; Murphy, R. B.; Repasky, M. P.; Frye, L. L.; Greenwood, J. R.; Halgren, T. A.; Sanschagrin, P. C.; Mainz, D. T., Extra precision glide: docking and scoring incorporating a model of hydrophobic enclosure for protein-ligand complexes. *J Med Chem* **2006,** *49* (21), 6177-96.
36. Halgren, T. A., Identifying and characterizing binding sites and assessing druggability. *J Chem Inf Model* **2009,** *49* (2), 377-89.
37. Beckstein, O.; Fourrier, A.; Iorga, B. I., Prediction of hydration free energies for the SAMPL4 diverse set of compounds using molecular dynamics simulations with the OPLS-AA force field. *J Comput Aided Mol Des* **2014,** *28* (3), 265-76.
38. Hoffmann, M. S., MITTELBIBERACH, 88441, DE), Grauert, Matthias (Osterbergstrasse 10, BIBERACH, 88400, DE), Breitfelder, Steffen (Weihergasse 21, ASSMANNSHARDT, 88433, DE), Eickmeier, Christian (Ayestrasse 10/2, MITTELBIBERACH, 88441, DE), Pohl, Gerald (Akazienweg 12, BIBERACH, 88400, DE), Lehmann-lintz, Thorsten (Ameisenberg 1, OCHSENHAUSEN, 88416, DE), Redemann, Norbert (Koehlesrain 48, BIBERACH, 88400, DE), Schnapp, Gisela (Esterbuch 5, BIBERACH-RINDENMOOS, 88400, DE), Steegmaier, Martin (Schloeglgasse 12/B5, WIEN, A-1120, AT), Bauer, Eckhart (Nickelshalde 11, BIBERACH, 88400, DE), Quant, Jens Jürgen (Hafergasse 32, GUNTRAMSDORF, A-2353, AT), NOVEL DIHYDROPTERIDINONES, METHOD FOR PRODUCING THE SAME AND THE USE THEREOF AS MEDICAMENTS. 2003.
39. Bradner, J. E. W., MA, US), Gray, Nathanael S. (Boston, MA, US), Qi, Jun (Sharon, MA, US), Mckeown, Michael R. (Brookline, MA, US), Buckley, Dennis (Boston, MA, US) DIHYDROPTERIDINONE DERIVATIVES AND USES THEREOF. 2016.
40. Sun, Q. Z.; Xu, Y.; Liu, J. J.; Zhang, C. H.; Wang, Z. R.; Zheng, R. L.; Wang, W. J.; Li, L. L.; Yang, S. Y., Structural modification of an EGFR inhibitor that showed weak off-target activity against RET leading to the discovery of a potent RET inhibitor. *Mol Divers* **2014,** *18* (2), 403-9.
41. Okumura, F. S.; Kusaka, H.; Takematsu, T., Studies on isokinetin and its analogs. I. Synthesis of isokinetin, 2-N-

furf
leaves. *J Biochem* **1961,** *49*, 133-7.

Supplementary Material

Schemes for alternative synthetic routes and mono-halogenated pteridinone analogs; tables of IC_{50} values for RSK inhibitors against the RSK1, 3, and 4 isoforms and for LJH685 and LJI308 against RSK2; Western blot of total and phosphor-RSK1 and RSK2 expression in leukemic cell lines; and inhibition of cellular RSK2 activity measured by nanoBRET assay.

Declaration of interests

☒ The authors declare that they have no known competing financial interests or personal relationships that could have appeared to influence the work reported in this paper.

☐The authors declare the following financial interests/personal relationships which may be considered as potential competing interests: